Measuring Distance between Reeb Graphs

Ulrich Bauer[*]   Xiaoyin Ge[†]   Yusu Wang[†]

September 29, 2016

Abstract

We propose a metric for Reeb graphs, called the functional distortion distance. Under this distance, the Reeb graph is stable against small changes of input functions. At the same time, it remains discriminative at differentiating input functions. In particular, the main result is that the functional distortion distance between two Reeb graphs is bounded from below by the bottleneck distance between both the ordinary and extended persistence diagrams for appropriate dimensions.

As an application of our results, we analyze a natural simplification scheme for Reeb graphs, and show that persistent features in Reeb graph remains persistent under simplification. Understanding the stability of important features of the Reeb graph under simplification is an interesting problem on its own right, and critical to the practical usage of Reeb graphs.

1   Introduction

One of the prevailing ideas in geometric and topological data analysis is to provide descriptors that encode useful information about hidden objects from observed data. The Reeb graph is one such descriptor. Specifically, given a continuous function $f : X \to \mathbb{R}$ defined on a domain X, the level set of f at value a is the set $f^{-1}(a) = \{x \in X \mid f(x) = a\}$. As the scalar value a increases, connected components appear, disappear, split and merge in the level set, and the Reeb graph of f tracks such changes. It provides a simple yet meaningful abstraction of the input domain. The concept behind the Reeb graph was first introduced by G. Reeb in [32] for Morse functions on manifolds; the term *Reeb graph* was coined by R. Thom. The first use of Reeb graphs for visualization applications can be found in work on shape understanding by Shinagawa et al. [33]. Since then, it has been used in a variety of applications in graphics and visualization, e.g, [25, 26, 29, 33, 35, 37]; also see [7] for a survey.

The Reeb graph can be computed efficiently in $O(m \log m)$ time for a piecewise-linear function defined on an arbitrary simplicial complex domain with m vertices, edges and triangles [30] (a randomized algorithm was given in [23]). This is in contrast to, for example, the $O(m^3)$ time (or matrix multiplication time) needed to compute even just the first-dimensional homology information for the same simplicial complex. The Reeb graph of a scalar field on a manifold can also be approximated from a point sample efficiently and with theoretical guarantees [17]. It encodes meaningful information on the input scalar field, in particular the so-called one-dimensional *vertical homology group* [17]. Being a graph structure, the Reeb graph is simple to represent and manipulate. These properties make the Reeb graph appealing for analyzing high-dimensional point data. For example, a generalization of the Reeb graph is proposed in [34] for analyzing high dimensional data, and in [22], the Reeb graph is used to recover a hidden geometric graph from its point samples. Very

---

[*]Department of Mathematics, Technical University of Munich (TUM), D-85747 Garching. http://ulrich-bauer.org

[†]Computer Science and Engineering Department, The Ohio State University, Columbus, OH 43221. Emails: gex, yusu@cse.ohio-state.edu.

recently in [10], it is shown that a certain Reeb graph can reconstruct a metric graph with respect to the Gromov-Hausdorff distance.

Given the popularity of the Reeb graph in data analysis, it is important to understand its stability and robustness with respect to changes in the input function (both in function values and in the domain). To measure the stability, we first need to define a distance between two Reeb graphs. Furthermore, an important application of the Reeb graph is to provide a descriptive summary of the function. Again, a central problem involved is to have a meaningful distance between Reeb graphs.

In the special case of Reeb graphs of functions on curves, similar results were obtained in [18] using an editing distance on Reeb graphs, and this approach is being extended to surfaces by the same authors. Recently, Morozov et al. proposed the *interleaving distance* for *merge trees*, based on the concept of an interleaving [11], and obtained similar upper and lower bounds relating this distance to *ordinary* persistence diagrams [28]. Here, the merge trees are variants of the loop-free Reeb graphs (*contour trees*). However, it is not clear how to generalize these results to Reeb graphs containing loops, an important family of features of the Reeb graph. Another distance based on the *branch decomposition* of merge trees was proposed in [6], together with a polynomial time algorithm to compute it. This distance, however, is not stable with respect to changes in the function and also does not generalize beyond trees.

Recently, de Silva et al. introduced the *interleaving distance* for Reeb graphs, which is defined at the algebraic topology level, utilizing the equivalence between Reeb graphs and a particular class of cosheaves [16]. In a previous conference paper [4], we introduced the functional distortion distance to be described in the current full version. Notably, it has been shown very recently in [5] that these two definitions of distances between Reeb graphs are strongly equivalent, in the sense that they are within constant factor of each other.

Our work. In this paper, we propose a metric for Reeb graphs, called the *functional distortion distance*, drawing intuition from the Gromov-Hausdorff distance for measuring metric distortion. Under this distance, the Reeb graph is stable against perturbations of the input function; at the same time, it retains a certain ability to discriminate between different functions (these statements will be made precise in Section 4). In particular, the main result is that the functional distortion distance between two Reeb graphs is bounded from below by (and thus more discriminative than) the *bottleneck distance* between the persistence diagrams *of the Reeb graphs*. On the other hand, the functional distortion distance yields the same type of sup norm stability that persistence diagrams enjoy [3, 11, 13, 14]. The persistence diagram has been a popular topological summary of shapes and functions, and the bottleneck distance is introduced in [14] as a natural distance for persistence diagrams. However, as the simple example in Fig. 1 (a) shows, the Reeb graph can be strictly more discriminative than the persistence diagram of dimension 0.

In Section 5, we show the relation between our functional distortion distance to a functional-version of the Gromov-Hausdorff distance. In Section 6, we show that, when applied to merge trees, our functional distortion distance is equivalent to the interleaving distance proposed by Morozov et al. [28].

Finally, as an application of our results, we show in Section 7 that persistent features of the Reeb graph remain persistent under a certain natural simplification strategy of the Reeb graph. Understanding the stability of Reeb graph features under simplification is an interesting problem on its own right: In practice, one often collapses small branches and loops in the Reeb graph to remove noise; see, e.g., [19, 22, 31]. It is crucial that by collapsing a collection of small features, there is no cascading effect that causes larger features to be destroyed, and our results confirm that this is indeed the case.

2   Preliminaries and Problem Definition

Reeb graphs. Given a continuous function $f : X \to \mathbb{R}$ on a finitely triangulable topological space X, for each $\alpha \in \mathbb{R}$, the set $f^{-1}(\alpha) = \{x \in X : f(x) = \alpha\}$ is called a *level set* of f. A level set may consist of several

connected components. We define an equivalence relation $\sim$ on X such that $x \sim y$ iff $f(x) = f(y) = \alpha$ and x is connected to y in $f^{-1}(\alpha)$. The *Reeb space* of the function $f : X \to \mathbb{R}$, denoted by R_f, is the quotient
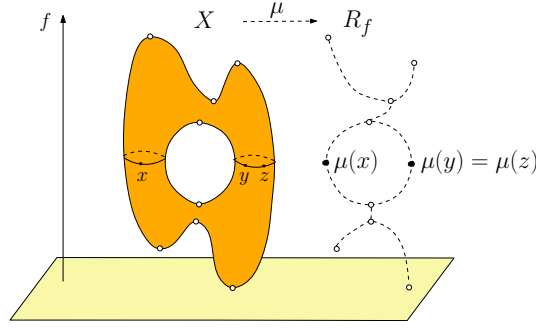
space $X/\sim$, i.e., the set of equivalent classes equipped with the quotient topology induced by the quotient map $\mu : X \to R_f$. Under appropriate regularity assumptions (to be made precise later), R_f has the structure of a finite 1-dimensional regular CW complex, and we call it a *Reeb graph*. Throughout this paper, we tacitly assume that all mentioned connected components are also path-connected.

The input function $f : X \to \mathbb{R}$ also induces a continuous function $\tilde{f} : R_f \to \mathbb{R}$ defined as $\tilde{f}(z) = f(x)$ for any preimage $x \in \mu^{-1}(z)$ of z. To simplify notation, we often write $f(z)$ instead of $\tilde{f}(z)$ for $z \in R_f$ when there is no ambiguity, and use $\tilde{f}$ mostly to emphasize the different domains of the functions. In all illustrations of this paper, we plot the Reeb graph with the vertical coordinate of a point z corresponding to the function value $f(z)$.

Given a point $x \in R_f$, we use the term *up-degree* (resp. *down-degree*) of x to denote the number of branches (1-cells) incident to x that have higher (resp. lower) values of f than x. A point is *regular* if both of its up-degree and down-degree equal to 1, and *critical* otherwise. A critical point is a minimum (maximum) if it has down-degree 0 (up-degree 0), and a down-fork (up-fork) if it has down-degree (up-degree) larger than 1. A critical point can be degenerate, having more than one types of criticality. From now on, we use the term *node* to refer to a critical point in the Reeb graph. For simplicity of exposition, we assume that all nodes of the Reeb graph have distinct $\tilde{f}$ function values. Note that because of the monotonicity of $\tilde{f}$ at regular points, the Reeb graph together with its associated function is completely described, up to homeomorphisms preserving the function, by the function values on the nodes.

Persistent homology and persistence diagrams. The notion of persistence was originally introduced by Edelsbrunner et al. in [21]. There has since been a great amount of development both in theory and in applications; see, e.g., [3, 9, 13, 38]. This paper does not concern the theory of persistence, hence we only provide a simple description so as to introduce the notion of *persistence diagrams*, which will be used later. We refer the readers to [24] for a detailed treatment of homology groups in general and to [20] for persistent homology.

Given a continuous function $f : X \to \mathbb{R}$ defined on a finitely triangulable topological space X, we call $X_{\leq a} = \{x \in X \mid f(x) \leq a\}$ a *sublevel set* of f. Let $H_p(Y)$ denote the p-th homology group of a triangulable topological space Y. Recall that a triangulation gives a CW structure and singular, simplicial, and cellular homology are isomorphic (see [24] for details). In this paper, we always consider homology with coefficients in $\mathbb{Z}_2$, so $H_p(Y)$ is a vector space. We now investigate the changes of $H_p(X_{\leq a})$ for increasing values of a. Throughout this paper, we will assume that f is *tame* in the following sense: there is a finite partition $-\infty = a_0 < \min f = a_1 < \cdots < a_N = \max f < \infty = a_{N+1}$ such that for all $i < n$ and $s, t \in [a_i, a_{i+1})$ with $s < t$, the homomorphism $H_p(X_{\leq s}) \to H_p(X_{\leq t})$ induced by the inclusion $X_{\leq s} \hookrightarrow X_{\leq t}$ is an isomorphism, and similarly, for all $s, t \in (a_i, a_{i+1}]$ with $s < t$, the homomorphism $H_p(X_{\geq t}) \to H_p(X_{\geq s})$ induced by the inclusion $X_{\geq t} \hookrightarrow X_{\geq s}$ is an isomorphism. Moreover, $H_p(X_{\leq a_i}) < \infty$ for all i. This implies that R_f is a Reeb graph. We call a_i a *homologically critical level* of f.
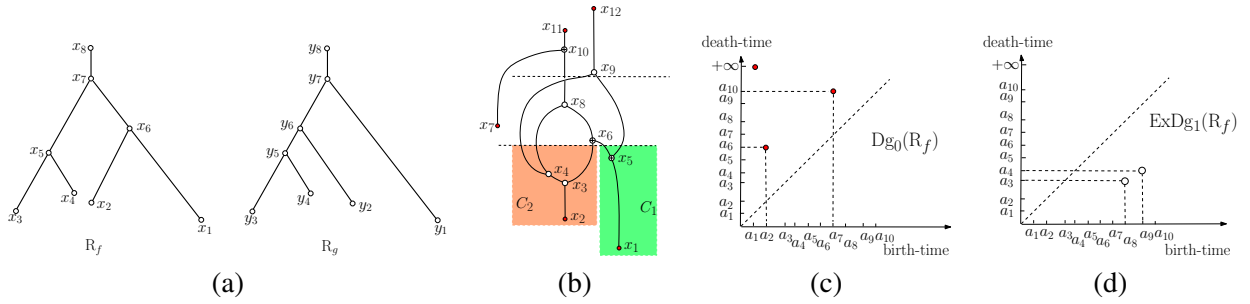
3

Figure 1: (a) The height functions on the two trees have the same persistence diagrams (thus the bottleneck distance between their persistence diagrams is 0), but their tree structures are different. The functional distortion distance will differentiate these two cases. In (b), solid dots are minimum and maximum, empty dots are essential forks, and crossed-dots are ordinary forks. The ordinary fork x_6 merges components C_1 and C_2 in the sublevel set below it, represented by minima x_1 and x_2 respectively. The resulting critical pair (x_2, x_6) gives rise to the point (a_2, a_6) in $\mathrm{Dg}_0(R_f)$ in (c), where $a_i = f(x_i)$ for $i \in [1, 12]$. The essential fork x_9 is paired with the up-fork x_4, corresponding to the thin loop $x_4 x_8 x_6 x_5 x_9 x_4$ created at x_9. This gives rise to the point (a_4, a_9) in the extended persistence diagram $\mathrm{ExDg}_1(R_f)$ in (d).

Consider the following sequence of vector spaces,

$$0 = H_p(X_{\leq a_0}) \to H_p(X_{\leq a_1}) \to \cdots \to H_p(X_{\leq a_N}) = H_p(X), \tag{1}$$

where each homomorphism $\mu_i^j : H_p(X_{\leq a_i}) \to H_p(X_{\leq a_j})$ is induced by the canonical inclusion $X_{\leq a_i} \hookrightarrow X_{\leq a_j}$.

A homology class h is created at a_i if

$$h \in H_p(X_{\leq a_i}) \text{ but } h \notin \mathrm{im}\, \mu_{i-1}^i.$$

It is destroyed at a_j if

$$\mu_i^{j-1}(h) \notin \mathrm{im}\, \mu_{i-1}^{j-1} \text{ but } \mu_i^j(h) \in \mathrm{im}\, \mu_{i-1}^j.$$

Persistent homology records such birth and death events. In particular, the p-th *ordinary persistence diagram* of f, denoted by $\mathrm{Dg}_p(f)$, is a multiset of pairs (b, d) corresponding' to the birth value b and death value d of some p-dimensional homology class. See Figure 1 (c) for an example of the 0-th persistence diagram. (We note that this is only an intuitive and informal introduction of the persistence diagram; see [20, 38] for a more formal treatment.)

In general, since $H_p(X)$ may not be trivial, any nontrivial homology class of $H_p(X)$, referred to as an *essential homology class*, will never die during the sequence in Eq. (1). For example, there is a point (a_1, ∞) in Fig. 1 (b) indicating a 0-dimensional homology class that was created at a_1 but never dies. By appending a sequence of relative homology groups to Eq. (1), we obtain a pairing of the essential homology classes (i.e., homology classes of $H_p(X)$):

$$0 = H_p(X_{\leq a_0}) \to \cdots \to H_p(X_{\leq a_N}) = H_p(X) =$$
$$H_p(X, X_{\geq a_N}) \to H_p(X, X_{\geq a_{N-1}}) \to \cdots \to H_p(X, X_{\geq a_0}) = 0. \tag{2}$$

Here $X_{\geq a}$ denotes the *superlevel set* $X_{\geq a} = \{x \in X \mid f(x) \geq a\}$. Since the last vector space $H_p(X, X_{\geq a_0}) = 0$, each essential homology class will necessarily die in the *relative part* of the above sequence at some relative homology group $H_p(X, X_{\geq a_j})$. We refer to the multiset of points encoding the birth and death time of pth homology classes created in the ordinary part and destroyed in the relative part of the sequence in Eq. (2) as the *pth extended persistence diagram* of f, denoted by $\mathrm{ExDg}_p(f)$. In particular, for each point (b, d) in

4

$\mathrm{ExDg}_p(f)$ there is a (essential) homology class in $H_p(X)$ that is born in $H_p(X_{\leq b})$ and dies at $H_p(X, X_{\geq d})$. See Fig. 1 (d) for an example; note that the birth time is larger than or equal to death time in the extended persistence diagram.

Reeb graphs and persistent homology. There is a natural way to define and quantify features of the Reeb graph, which turns out to be consistent with the information encoded in the diagrams $\mathrm{Dg}_0(R_f)$ and $\mathrm{ExDg}_1(R_f)$ of the function $\tilde{f} : R_f \to \mathbb{R}$. Since R_f is a graph, we only need to consider persistent homology in dimensions 0 and 1. We provide an intuitive treatment below. For simplicity of exposition, we assume that all nodes have different function values and are either a minimum, a maximum, a down-fork with down-degree 2, or an up-fork with up-degree 2, noting that these assumptions hold in the generic case.

Imagine that we sweep through R_f in increasing values of a and inspect changes in $H_0((R_f)_{\leq a})$. New components in the *sublevel sets* are created at minima of R_f. For any value a, associate each component C in the sublevel set of $(R_f)_{\leq a}$ with the lowest local minimum m contained in C: intuitively, C is created at m.

Consider a down-fork node s with $a = f(s)$. If the two lower branches are contained in different connected components C_1 and C_2 of the open sublevel set $(R_f)_{<a}$, for reasons that will become obvious soon we call s an *ordinary fork*; otherwise, it is an *essential fork*. Let x_1 and x_2 be the global minimum of C_1 and C_2, respectively. Assume that $f(x_1) < f(x_2)$. Then the homology class $[x_2 + x_1]$ is created at $f(x_2)$ and dies at $f(s)$, giving rise to a unique point $(f(x_2), f(s))$ in the 0-th ordinary persistence diagram $\mathrm{Dg}_0(R_f)$. Indeed, there is a one-to-one correspondence between the set of such pairs of minima and ordinary down-forks and points in the 0th persistence diagram $\mathrm{Dg}_0(R_f)$ with finite coordinates; see Fig. 1 (b) and (c). A symmetric procedure with $-f$ will produce pairs of maxima and ordinary up-forks, corresponding to points in the 0th persistence diagram $\mathrm{Dg}_0(R_{-f})$. Together, these pairs capture the *branching features* of a Reeb graph.

If, on the other hand, the two lower branches of s are connected in the sublevel set, we call s an *essential fork*; see Fig. 1 (b) and (d). In this case, some cellular 1-cycle in the sublevel set $(R_f)_{\leq a}$ is born at a. Since R_f is a graph, this cycles is non-trivial in R_f, and their corresponding homology classes will not be destroyed in ordinary persistent homology. Consider the unique cycle γ with largest minimum value of f among all cycles born at a and corresponding to an embedded loop in R_f. Let s' be the point achieving the minimum on γ. Then the cycle γ is created at $f(s)$ during the ordinary sequence of Eq. (2), and killed at time $f(s')$ in the extended part, giving rise to a unique point $(\tilde{f}(s'), \tilde{f}(s))$ in the 1st extended persistence diagram of $\tilde{f}$. It turns out that s' is necessarily an essential up-fork [1], and we call such a pair (s', s) an *essential pair*. Indeed, the collection of essential pairs has a one-to-one correspondence to points in $\mathrm{ExDg}_1(R_f)$. (The extended persistence diagram $\mathrm{ExDg}_1(R_{-f})$ is the reflection of $\mathrm{ExDg}_1(R_f)$ and thus encodes the same information as $\mathrm{ExDg}_1(R_f)$.) These essential pairs capture the *cycle features* of a Reeb graph.

In short, the branching features and cycle features of a Reeb graph give rise to points in the 0th ordinary and 1st extended persistence diagrams, respectively. However, the persistence diagram captures only the lifetime of features, but not how these features are connected; see Fig. 1 (a). In this paper we aim to develop a way of measuring distance between Reeb graphs which also takes into account the graph structure.

3   A Metric on Reeb Graphs

Throughout this paper, by a *distance* we will mean an extended pseudometric, i.e., a binary symmetric function d with values in $[0, \infty]$ that satisfies $d(x, x) = 0$ and $d(x, z) \leq d(x, y) + d(y, z)$. From now on, consider two Reeb graphs R_f and R_g, generated by tame functions $f : X \to \mathbb{R}$ and $g : Y \to \mathbb{R}$. While topologically each Reeb graph is simply a 1-dimensional regular CW complex, it is important to note that it also has a function associated with it (induced from the input scalar field). Hence the distance should depend on both the graph structures and the functions $\tilde{f}$ and $\tilde{g}$. Approaching the problem through graph isomorphisms does not seem viable, as small perturbation of the function f may create an arbitrary number of new branches and

loops in the graph. To this end, we first put the following metric structure on a Reeb graph R_f to capture information about the function f.

Specifically, for any two points $u, v \in R_f$ (not necessarily nodes), let π be a continuous path between u and v. The *range* of this path is the interval $\text{range}(\pi) := [\min_{x \in \pi} f(x), \max_{x \in \pi} f(x)]$, and its *height* is simply the length of the range, denoted by $\text{height}(\pi) = \max_{x \in \pi} f(x) - \min_{x \in \pi} f(x)$. We define the distance

$$d_f(u, v) = \min_{\pi : u \rightsquigarrow v} \text{height}(\pi), \tag{3}$$

where π ranges over all paths from u to v, denoted by $u \rightsquigarrow v$. Equivalently, $d_f(u, v)$ is the minimum length of any interval I such that u and v are in the same connected component of $f^{-1}(I)$. Note that this is in fact a metric, since on Reeb graphs there is no path of constant function value between two points $u \neq v$. We put f in the subscript to emphasize the dependency on the input function. Intuitively, $d_f(u, v)$ is the minimal function difference one has to overcome to move from u to v.

To define a distance between R_f and R_g, we need to connect the spaces R_f and R_g, which is achieved by continuous maps $\phi : R_f \to R_g$ and $\psi : R_g \to R_f$. Borrowing from the definition of Gromov–Hausdorff distance given in [27], let

$$G(\phi, \psi) = \{(x, \phi(x)) : x \in R_f\} \cup \{(\psi(y), y) : y \in R_g\} \text{ and}$$

$$D(\phi, \psi) = \sup_{(x,y),(\tilde{x},\tilde{y}) \in G(\phi, \psi)} \frac{1}{2} \left| d_f(x, \tilde{x}) - d_g(y, \tilde{y}) \right|, \tag{4}$$

where $G(\phi, \psi)$, the union of the graphs of ϕ and ψ, can be thought of as the set of correpondences between R_f and R_g induced by maps ϕ and ψ. The *functional distortion distance* is defined as:

$$d_{FD}(R_f, R_g) = \inf_{\phi, \psi} \max \{D(\phi, \psi), \|f - g \circ \phi\|_\infty, \|f \circ \psi - g\|_\infty\}, \tag{5}$$

where ϕ and ψ range over all continuous maps between R_f and R_g. The latter two terms address the fact that composition with isometries of the real line (translation, negation) does not affect the metric d_f induced by a function f. Note that this definition can be considered as a continuous, functional variant of the Gromov–Hausdorff distance, with the additional condition that the maps between R_f and R_g are required to be continuous, and taking into consideration the difference between the function values of corresponding points as well. In fact, this definition is the continuous version of the extended Gromov-Hausdorff distance introduced in Definition 2.4 of [12]. Furthermore, it turns out that for metric graphs, our continuous version of the extended Gromov-Hausdorff (GH) distance is a constant factor approximation of the extended GH distance induced by arbitrary maps, which we will make precise and show later in Section 5. As an example, consider the two trees in Fig. 1. The distortion of distances in the two trees in (a) is large no matter how we identify correspondences between points from them. Thus the functional distortion distance between them is also large, making it more discriminative than the bottleneck distance between persistence diagrams.

It is straightforward to show that the functional distortion distance is a pseudometric, and a metric on the equivalence classes of Reeb graphs up to function-preserving homeomorphisms. Note that this definition and our results apply to any graph G with a function f that is strictly monotonic on the edges. This is easy to see since in that case $R_f = G$ and $\tilde{f} = f$.

4   Properties of the Functional Distortion Distance

In this section, we show that the functional distortion distance is both stable (upper bounded) and discriminative (lower bounded). Note that it is somewhat meaningless to discuss the stability of a distance alone without understanding its discriminative power – the constant function with value 0 is a pseudo-metric too.

4.1 Stability

Suppose that f and g are defined on the same domain X. Furthermore, assume that the quotient maps μ_f and μ_g have continuous sections (right-inverses) s_f and s_g, i.e., $\mu_f \circ s_f = \text{id}_{R_f}$ and $\mu_g \circ s_f = \text{id}_{R_f}$. Then we have the following stability result for the metric d_{FD} for Reeb graphs.

Theorem 4.1. *Let $f, g : X \to \mathbb{R}$ be tame functions whose Reeb quotient maps $\mu_f : X \to R_f$ and $\mu_g : X \to R_g$ have continuous sections. Then $d_{FD}(R_f, R_g) \leq \|f - g\|_\infty$.*

Proof. Let $\delta = \|f - g\|_\infty$. Choose $\phi = \mu_g \circ s_f, \psi = \mu_f \circ s_g$. Now assume that $(x, y), (\tilde{x}, \tilde{y}) \in G(\phi, \psi)$, with $G(\phi, \psi)$ as defined in Eq. (4). Let $\xi = s_f(x), \tilde{\xi} = s_f(\tilde{x}), \upsilon = s_g(y)$, and $\tilde{\upsilon} = s_g(\tilde{y})$. Note that either $y = \phi(x)$ or $x = \psi(y)$, so either

$$\mu_g(\upsilon) = y = \phi(x) = \mu_g \circ s_f(x) = \mu_g(\xi)$$

or

$$\mu_f(\xi) = x = \psi(y) = \mu_f \circ s_g(y) = \mu_f(\upsilon).$$

In other words, ξ and υ are either in the same level set component of f or of g, and analogously for $\tilde{\xi}$ and $\tilde{\upsilon}$.

Let $[a, b]$ be such that $x, \tilde{x}$ are connected in $\tilde{f}^{-1}[a, b]$. Then ξ and $\tilde{\xi}$ are connected in

$$f^{-1}[a, b] \subset g^{-1}[a - \delta, b + \delta],$$

and hence, by the above, υ and $\tilde{\upsilon}$ are also connected in $g^{-1}[a - \delta, b + \delta]$. Therefore, y and $\tilde{y}$ are connected in $\tilde{g}^{-1}[a - \delta, b + \delta]$. We conclude that $(b - a) + 2\delta \geq d_g(y, \tilde{y})$. Since this inequality holds for all intervals $[a, b]$ with the stated properties, we have $d_f(x, \tilde{x}) + 2\delta \geq d_g(y, \tilde{y})$. By symmetry of the above argument, we also have $d_g(y, \tilde{y}) + 2\delta \geq d_f(x, \tilde{x})$. Moreover, by assumption,

$$\max_{x \in R_f} |f(x) - g \circ \phi(x)| \leq \max_{y \in X} |f(y) - g(y)| = \delta.$$

Similarly,

$$\max_{x \in R_g} |g(x) - f \circ \psi(x)| \leq \max_{y \in X} |g(y) - f(y)| = \delta.$$

Hence $\|f - g \circ \phi\|_\infty \leq \delta$ and $\|f \circ \psi - g\|_\infty \leq \delta$. Combining these with Eq. (5), we conclude that $d_{FD}(R_f, R_g) \leq \|f - g\|_\infty$. □

The above result is similar to the stability result obtained for the bottleneck distance between persistence diagrams [15], as well as for the ε-interleaving distance between merge trees [28]. Note that the above stated conditions (on the existence of continuous sections) are only required for the stability result. They are not necessary for Theorems 4.2 and 4.3. The condition on the common domain X is required so that we can define the distance between input scalar fields f and g. The condition on the existence of sections is purely technical; it holds e.g. for Morse functions or for generic PL functions.

4.2 Relation to Ordinary Persistence Diagram

The main part of this section is devoted to discussing the discriminative power of the functional distortion distance for Reeb graphs. In particular, we relate this distance with the bottleneck distance between persistence diagrams. We have already seen in Fig. 1 (a) that there are cases where the functional distortion distance is strictly larger than the bottleneck distance between persistence diagrams of according dimensions (0th ordinary and 1st extended persistence diagrams). We next show that, up to a constant factor, the functional distortion distance is always at least as large as the bottleneck distance. We take different approaches to investigate the branching features (ordinary persistence diagram) and the cycle features (extended persistence diagram). For the former, we have the following main result. The proof is rather standard, and similar to the result on interleaving distance between merge trees in [28].

Theorem 4.2. $d_B(\mathrm{Dg}_0(R_f), \mathrm{Dg}_0(R_g)) \le d_{FD}(R_f, R_g)$. *Similarly, $d_B(\mathrm{Dg}_0(R_{-f}), \mathrm{Dg}_0(R_{-g})) \le d_{FD}(R_f, R_g)$.*

Proof. Let $\phi : R_f \to R_g$ and $\psi : R_g \to R_f$ be the optimal continuous maps that achieve $\delta = d_{FD}(R_f, R_g)$ [1]. First, note that by Eq. (5), $\max_{x \in R_f} |f(x) - g(\phi(x))| \le \delta$. Hence $\phi : (R_f)_{\le \alpha} \to (R_g)_{\le \alpha + \delta}$ is well defined for any $\alpha \in \mathbb{R}$. Similarly, $\psi : (R_g)_{\le \beta} \to (R_f)_{\le \beta + \delta}$ is well defined for any $\beta \in \mathbb{R}$. Let i denote the canonical inclusion maps, and for any map ρ, let ρ_* indicate the induced homomorphism on homology. We now show that the following diagram commutes for any real value α:

$$H_0\left((R_f)_{\le \alpha}\right) \xrightarrow{\ i_* \ } H_0\left((R_f)_{\le \alpha + 2\delta}\right)$$
$$\phi_* \searrow \quad \nearrow \psi_*$$
$$H_0\left((R_g)_{\le \alpha + \delta}\right)$$

To show the commutativity of the above diagram, we need to show that for any 0-cycle c in $(R_f)_{\le \alpha}$, $[i(c)] = [\psi \circ \phi(c)]$, where $[c']$ is the homology class represented by a cycle c'. Assume w.l.o.g. that the 0-cycle $c = x_1 + x_2$ contains only two points x_1, x_2 from $(R_f)_{\le \alpha}$; the argument easily extends to the case where c contains an arbitrary even number of points. Let $x_1' = \psi \circ \phi(x_1)$ and $x_2' = \psi \circ \phi(x_2)$. Since $d_f(x_1, x_1') \le \delta$, we know that there is a path (1-chain) $\pi(x_1, x_1')$ with height at most δ connecting x_1 and x_1'. In other words, x_1 and x_1' are connected in $(R_f)_{\le \alpha + \delta} \subseteq (R_f)_{\le \alpha + 2\delta}$. Similarly, x_2 and x_2' are connected in $(R_f)_{\le \alpha + 2\delta}$. Hence the new 0-cycle $c' = x_1' + x_2' = \psi \circ \phi(c)$ is homologous to c in $(R_f)_{\le \alpha + 2\delta}$. Thus, $[i(c)] = [c'] = [\psi \circ \phi(c)]$.

A similar argument also shows that the symmetric versions of the diagrams in Footnote 1 (by switching the roles of R_f and R_g) also commute at the 0th homology level. This means that the two persistence modules $\{H_0((R_f)_{\le \alpha})\}_\alpha$ and $\{H_0((R_g)_{\le \beta})\}_\beta$ are strongly δ-interleaved (as introduced in [11]). The first half of Theorem 4.2 then follows from Theorem 4.8 of [11].

The same argument works for the scalar fields $-\tilde{f} : R_f \to \mathbb{R}$ and $-\tilde{g} : R_g \to \mathbb{R}$, which proves the second half of Theorem 4.2. Recall that $\mathrm{Dg}_0(R_f)$ captures minimum and down-fork persistence pairs, while $\mathrm{Dg}_0(R_{-f})$ captures up-fork and maximum persistence pairs. $\square$

4.3 Relation to Extended Persistence Diagram

Recall that the range of cycle features in the Reeb graph correspond to points in the 1st extended persistence diagram. In what follows we will show the following main theorem, which states that $d_{FD}(R_f, R_g)$ is bounded below by the bottleneck distance between the 1st extended persistence diagrams $\mathrm{ExDg}_1(R_f)$ and $\mathrm{ExDg}_1(R_g)$.

Theorem 4.3. $d_B(\mathrm{ExDg}_1(R_f), \mathrm{ExDg}_1(R_g)) \le 3 d_{FD}(R_f, R_g)$.

For simplicity of exposition, we assume that $d_{FD}(R_f, R_g)$ can be achieved by optimal continuous maps $\phi : R_f \to R_g$ and $\psi : R_g \to R_f$. The case where $d_{FD}(R_f, R_g)$ is achieved in the limit can be handled by considering a sequence of continuous maps that are optimal up to an arbitrarily small additive term ϵ. Let $\delta = d_{FD}(R_f, R_g)$.

Thin bases. Let $Z_1(R_f)$ be the 1-dimensional cellular cycle group of R_f with coefficients in $\mathbb{Z}_2$, i.e., the subgroup of the 1-dimensional cellular chains with zero boundary. Since the Reeb graph has the structure of a 1-dimensional CW complex, the 1-dimensional cellular boundary group is trivial, and so every *cellular* 1-cycle of R_f represents a unique homology class[2] in $H_1(R_f)$; that is, $H_1(R_f) \cong Z_1(R_f)$.

For a cellular 1-cycle $\gamma = \sum_\alpha e_\alpha$, let im γ denote the union of the images of the characteristic maps for all 1-cells (edges) e_α. Let $\mathrm{range}(\gamma) = [\min_{x \in \mathrm{im}\,\gamma} f(x), \max_{x \in \mathrm{im}\,\gamma} f(x)]$ denote the *range* of a cycle γ, and let

---

[1] If the $d_{FD}(R_f, R_g)$ is achieved only in the limit, then one can extend the argument by constructing two sequences of maps that are optimal up to an arbitrarily small additive term ε and taking the limit in the distance they induce.

[2] Note that the same is not true for singular homology; this is the reason why we consider cellular cycles here.

height(γ) be the length of this interval. A cycle is *thinner* than another one if its height is strictly smaller. A cycle γ is *thin* if it cannot be written as a linear combination of thinner cycles. See Fig. 1 (b), where the cycle $x_4x_8x_6x_5x_9x_4$ is thin, while the cycle $x_3x_4x_9x_5x_6x_3$ is not. Given a basis of $Z_1(R_f)$, consider the sequence of the heights of the cycles contained in it, ordered in non-decreasing order. A basis for $Z_1(R_f)$ is a *thin* basis if its height sequence is less than or equal to that of any other basis of $Z_1(R_f)$ in the lexicographic order. Obviously, each cycle in a thin basis is necessarily a thin cycle.

From now on, we fix an arbitrary thin basis $\mathcal{G}_f = \{\gamma_1, \ldots, \gamma_n\}$ of $Z_1(R_f)$ and $\mathcal{G}_g = \{\zeta_1, \ldots, \zeta_m\}$ of $Z_1(R_g)$, with n and m being the rank of $Z_1(R_f)$ and $Z_1(R_g)$, respectively. It is known [15] that every cycle in a thin basis of R_f is necessarily a thin cycle, and the ranges $[b, d]$ of cycles in $\mathcal{G}_f$ (resp. in $\mathcal{G}_g$) correspond one-to-one to the points (b, d) in the 1st extended persistence diagram $\text{ExDg}_1(R_f)$ (resp. in $\text{ExDg}_1(R_g)$). For example, in Fig. 1 (b), the two cycles $x_3x_4x_8x_6x_3$ and $x_4x_8x_6x_5x_9x_4$ form a thin basis, corresponding to points $(\tilde{f}(x_8), \tilde{f}(x_3))$ and $(\tilde{f}(x_9), \tilde{f}(x_4))$ in $\text{ExDg}_1(R_f)$ in (d).

Given any cycle γ of R_f (resp. of R_g), we can represent γ uniquely as a linear combination of cycles in $\mathcal{G}_f$ (resp. $\mathcal{G}_g$), which we call the *thin basis decomposition of γ*; we omit the reference to $\mathcal{G}_f$ and $\mathcal{G}_g$ since they will be fixed from now on. The thin cycle with the largest height from the thin basis decomposition of γ is called the *dominating cycle of γ*, denoted by $\text{dom}(\gamma)$. If there are multiple cycles with the same maximal height, then by convention we choose the one with smallest index in $\mathcal{G}_f$ (resp. in $\mathcal{G}_g$) as the dominating cycle. A cycle γ is *α-stable* if its dominating cycle has a height strictly larger than 2α. Let $Z_1^\alpha(R_f)$ denote the subgroup of $Z_1(R_f)$ generated by cycles with height at most 2α. Equivalently, a thin basis decomposition of a cycle in $Z_1^\alpha(R_f)$ consists only of cycles with height at most 2α. Hence, a cycle z is in $Z_1^\alpha(R_f)$ if and only if z is *not* α-stable. Note that this only means that the *dominating* cycle of z has height at most 2α; the height of z itself can be larger than 2α. We have the following property of the dominating cycle:

Lemma 4.4. *A set of cycles $\gamma_1, \ldots \gamma_k \in Z_1(R_f)$ with distinct dominating cycles is linearly independent.*

Proof. We show that $\sum_{j=1}^a \gamma_{i_j} \neq 0$ for any subset $\{i_1, \ldots, i_a\} \subseteq \{1, 2, \ldots, k\}$. Specifically, consider the maximum height of dominating cycles of any cycle in $\{\gamma_{i_j}\}_{j=1}^a$. First, assume that there is only a unique cycle, say γ_{i_a}, whose dominating cycle $\text{dom}(\gamma_{i_a})$ has this maximum height. It then follows that this thin cycle $\text{dom}(\gamma_{i_a})$ is not in the thin basis decomposition of any other cycle γ_{i_j}, $j \neq a$. Since the thin basis decomposition of the cycle $\sum_{j=1}^a \gamma_{i_j}$ is simply the sum (modulo 2) of thin basis decomposition of each γ_{i_j}, $\text{dom}(\gamma_{i_a})$ must exist in the thin basis decomposition of the cycle $\sum_{j=1}^a \gamma_{i_j}$; in fact, $\text{dom}(\sum_{j=1}^a \gamma_{i_j}) = \text{dom}(\gamma_{i_a})$. Therefore $\sum_{j=1}^a \gamma_{i_j} \neq 0$.

If there are multiple cycles whose dominating cycle has the maximal height, then we consider the one whose dominating cycle has the smallest index among all of them. The same argument as above shows that this cycle will present in the thin basis decomposition of the cycle $\sum_{j=1}^a \gamma_{i_j}$, implying that $\sum_{j=1}^a \gamma_{i_j} \neq 0$. □

α-matching. The main use of thin cycles is that we will prove Theorem 4.3 by showing the existence of an *α-matching* between $\mathcal{G}_f$ and $\mathcal{G}_g$. Specifically, two thin cycles γ_1 and γ_2 are *α-close* if their ranges $[a, b]$ and $[c, d]$ are within Hausdorff distance α, i.e., $|c - a| \leq \alpha$ and $|d - b| \leq \alpha$. (Note that two α-close cycles can differ in height by at most 2α.) An *α-matching* for $\mathcal{G}_f$ and $\mathcal{G}_g$ is a set of pairs $\mathcal{M} \subset \mathcal{G}_f \times \mathcal{G}_g$ such that:

(I) For each pair $(\gamma, \zeta) \in \mathcal{M}$, the cycles γ and ζ are α-close; and

(II) Every α-stable cycle in $\mathcal{G}_f$ and $\mathcal{G}_g$ (i.e., with height larger than 2α) appears in *exactly one* pair of $\mathcal{M}$; every other cycle appears in at most one pair.

Since each point (b, d) in the extended persistence diagram corresponds to the range $[b, d]$ of a unique cycle in a given thin basis, $d_B(\text{ExDg}_1(R_f), \text{ExDg}_1(R_g)) \leq \alpha$ if and only if there is an α-matching for $\mathcal{G}_f$ and $\mathcal{G}_g$. Our goal now is to prove that there exists a 3δ-matching for $\mathcal{G}_f$ and $\mathcal{G}_g$, which will then imply Theorem 4.3.

Properties of ϕ and ψ. Recall that $\phi : R_f \to R_g$ and $\psi : R_g \to R_f$ are the optimal continuous maps that

9

achieve $\delta = d_{FD}(R_f, R_g)$. We now investigate the effect of these maps on thin cycles. Note that ϕ and ψ induce maps $Z_1(R_f) \to Z_1(R_g)$ and $Z_1(R_g) \to Z_1(R_f)$. To simplify notation, we denote these maps by ϕ and ψ as well. Lemma 4.5 below states that ψ is "close" to being an inverse of ϕ. Lemmas 4.6 and 4.7 relate the range of $\phi(\gamma)$ with the range of γ.

Lemma 4.5. *Given any cycle $\gamma \in Z_1(R_f)$, we have $\psi \circ \phi(\gamma) \in \gamma + Z_1^{2\delta}(R_f)$. That is, $\psi \circ \phi(\gamma) = \gamma + \gamma'$, where γ' is not 2δ-stable. A symmetric statement holds for any cycle in R_g.*

Proof. The input Reeb graph R_f is a finite graph, and there are only a finite number of (cellular) cycles. Hence there are only a finite number of height values (reals) that these cycles can have. Let α denote the lowest height of any cycle whose height is strictly larger than 4δ. We set ρ to be any positive constant between 0 and $\alpha - 4\delta$; that is, $4\delta + \rho < \alpha$. Note that if a cycle γ satisfies height(γ) $\leq 4\delta + \rho < \alpha$, then it is necessary that height(γ) $\leq 4\delta$.

Assume that im γ has only a single connected component – the case with multiple components can be handled in a component-wise manner. This means that γ is generated by a loop ℓ, i.e., a closed curve on R_f, in the sense that we can consider ℓ as a singular cycle and then use the isomorphism of singular homology and cellular cycles. Without loss of generality, we may assume that ℓ is embedded; otherwise, ℓ can be split into embedded subloops, which again can be treaded separately. Now for the given loop ℓ, let $\tilde{\ell}$ denote $\psi \circ \phi(\ell)$, and for any point x on ℓ, let $\tilde{x} \in \tilde{\ell}$ denote $\tilde{x} := \psi \circ \phi(x)$. Since both $(x, \phi(x))$ and $(\tilde{x}, \phi(x))$ are in $G(\phi, \psi)$, by Eq. (5), there is an embedded path $\pi(x, \tilde{x})$ connecting x to $\tilde{x}$ with range($\pi(x, \tilde{x})$) = $[a, b]$, where $b - a \leq 2\delta$.

Let $\ell[x, x']$ and $-\ell[x, x']$ denote the orientation-preserving and orientation-reversing subcurves of ℓ from x to x', respectively. Start with an arbitrary point $x = x_0$ on ℓ, and consider $\tilde{x}_0$ on $\tilde{\ell}$. Since $\psi \circ \phi$ is a continuous map, as we move x along ℓ continuously, $\tilde{x}$ moves continuously. In step i, as we move along ℓ (starting from x_i), we set x_{i+1} to be the first point such that the height of the loop $\ell_i = \ell[x_i, x_{i+1}] \circ \pi(x_{i+1}, \tilde{x}_{i+1}) \circ -\tilde{\ell}[\tilde{x}_{i+1}, \tilde{x}_i] \circ \pi(\tilde{x}_i, x_i)$ is $4\delta + \rho$. If no such ℓ_i exists before $\tilde{x}$ moves back to $\tilde{x}_0$, then we set x_{i+1} to be x_0, and the process terminates. Since both $\pi(x_{i+1}, \tilde{x}_{i+1})$ and $\pi(\tilde{x}_i, x_i)$ are paths of height at most 2δ, the sum of the heights of $\ell[x_i, x_{i+1}]$ and $-\tilde{\ell}[\tilde{x}_i, \tilde{x}_{i+1}]$ must be at least ρ. Hence, for a fixed value ρ, this process terminates in a finite number of steps. Now let c_i denote the cellular cycle homologous to the loop ℓ_i in the above construction. By construction, we have that $\gamma = \tilde{\gamma} + \sum_i c_i$, where $\tilde{\gamma} = \psi \circ \phi(\gamma)$. Since each c_i satisfies height(c_i) $\leq$ height(ℓ_i) $\leq 4\delta + \rho < \alpha$, as discussed earlier it then follows that height(c_i) $\leq 4\delta$. Hence $c_i \in Z_1^{2\delta}(R_f)$ for each i and $\gamma' = \sum_i c_i \in Z_1^{2\delta}(R_f)$, implying that $\psi \circ \phi(\gamma) = \tilde{\gamma} = \gamma + \gamma' \in \gamma + Z_1^{2\delta}(R_f)$. $\square$

Lemma 4.6. *Given any thin cycle $\gamma \in Z_1(R_f)$ with range $[b, d]$, we have that the range of any cycle in the thin basis decomposition of $\phi(\gamma)$ must be contained in the interval $[b - \delta, d + \delta]$.*

Proof. First, by Eq. (5), we have $\max_{x \in R_f} |f(x) - g(\phi(x))| \leq \delta$. Hence range($\phi(\gamma)$) $\subseteq [b - \delta, d + \delta]$. Now let b' be the smallest left endpoint of the range of any cycle in the thin basis decomposition of $\phi(\gamma)$. We will prove that $b' \geq b - \delta$.

Suppose this is not case and $b' < b - \delta$. Now let $\zeta_{i_1}, \ldots, \zeta_{i_a} \in \mathcal{G}_g$, $a \geq 1$, denote all those cycles in the thin basis decomposition of $\phi(\gamma)$ whose ranges have b' as the left endpoint. Set $\rho = \zeta_{i_1} + \cdots \zeta_{i_a}$. Assume ζ_{i_a} has the largest height among these thin cycles. Note that range(ζ_{i_j}) $\subseteq$ range(ζ_{i_a}) for any $j < a$, as all these ranges share the same left endpoint b'. Clearly range(ρ) $\subseteq$ range(ζ_{i_a}). On the other hand, by definition of b' and ζ_{i_j}, all other cycles in the thin basis decomposition of $\phi(\gamma)$ have a range whose left endpoint is strictly greater than b'. Let ρ' be the sum of these other cycles; we have that $\phi(\gamma) = \rho + \rho'$. Since the left endpoint of range(ρ') is strictly bigger than b', the left endpoint of range(ρ) also has to be strictly bigger than b', as otherwise the left endpoint of range($\rho + \rho'$) would be b', which contradicts to the fact that the left endpoint of range($\phi(\gamma)$) is at least $b - \delta > b'$. In other words, it is necessary that range(ρ) is a proper subset of range(ζ_{i_a}); i.e., range(ρ) $\subset$ range(ζ_{i_a}). This implies that ρ has strictly smaller height than ζ_{i_a}. This however contradicts that $\mathcal{G}_g$ is a thin basis, because we can replace ζ_{i_a} in $\mathcal{G}_g$ with ρ and obtain a basis element with smaller height (the resulting set of cycles remain independent). Therefore it is not possible that $b' < b - \delta$.

10

A symmetric argument shows that the largest right endpoint of the range of any cycle in the thin basis decomposition of $\phi(\gamma)$ is at most $d + \delta$. Hence the range of any cycle in the thin basis decomposition of $\phi(\gamma)$ is a subset of $[b - \delta, d + \delta]$. $\qquad\square$

Lemma 4.7. *For any 2δ-stable cycle $\gamma \in Z_1(R_f)$, we have*

$$\text{height}(\text{dom}(\phi(\gamma))) \geq \text{height}(\text{dom}(\gamma)) - 2\delta.$$

A symmetric statement holds for any cycle of R_g.

Proof. Note that in this lemma, γ is not necessarily a thin loop. Let $\gamma_s = \text{dom}(\gamma)$; since γ is 2δ-stable, we have height$(\gamma_s) > 4\delta$. First, we claim that dom$(\psi \circ \phi(\gamma)) = \gamma_s$. This is because by Lemma 4.5, $\psi \circ \phi(\gamma) \in \gamma + Z_1^{2\delta}(R_f)$. Since height$(\gamma_s) > 4\delta$, γ_s still belongs to the thin basis decomposition of $\psi \circ \phi(\gamma)$ and still has the largest height.

Now set $\tilde{\zeta} = \phi(\gamma)$ with $\zeta_{i_1} + \cdots + \zeta_{i_a}$ being its thin basis decomposition. Observe that for any cycle γ' in R_f, we have that height$(\phi(\gamma')) \leq$ height$(\gamma') + 2\delta$, which follows from the fact that for any $x \in R_f$, $|f(x) - g(\phi(x))| \leq \delta$; recall Eq. (5). A symmetric statement holds for a loop from R_g. We thus have:

$$\text{height}(\text{dom}(\psi(\tilde{\zeta}))) = \text{height}(\text{dom}(\sum_{j=1}^{a} \psi(\zeta_{i_j}))) \leq \max_{j=1}^{a} \text{height}(\psi(\zeta_{i_j}))$$

$$\leq \max_{j=1}^{a} [\text{height}(\zeta_{i_j}) + 2\delta] = \max_{j=1}^{a} \text{height}(\zeta_{i_j}) + 2\delta$$

$$= \text{height}(\text{dom}(\tilde{\zeta})) + 2\delta. \tag{6}$$

Since we have shown earlier that dom$(\psi \circ \phi(\gamma)) = \gamma_s$, it follows that dom$(\psi(\tilde{\zeta})) = \text{dom}(\psi \circ \phi(\gamma)) = \gamma_s = \text{dom}(\gamma)$. Combining this with Eq. (6), we have

$$\text{height}(\text{dom}(\phi(\gamma))) = \text{height}(\text{dom}(\tilde{\zeta})) \geq \text{height}(\text{dom}(\psi(\tilde{\zeta}))) - 2\delta$$

$$= \text{height}(\text{dom}(\gamma)) - 2\delta,$$

which proves the lemma. $\qquad\square$

In fact, if γ is a thin cycle, Lemma 4.7 can be strengthened to show that dom$(\phi(\gamma))$ is δ-close to γ. This already provides some mapping of base cycles from $\mathcal{G}_f$ to cycles from $\mathcal{G}_g$ such that each pair of corresponding cycles are δ-close. However, the main challenge is to show that there exists a *one-to-one* correspondence for all 3δ-stable cycles (recall the definition of a 3δ-matching of $\mathcal{G}_f$ and $\mathcal{G}_g$). For this, we need to take a slight detour to relate cycles in $\mathcal{G}_f$ with those in $\mathcal{G}_g$ in a stronger sense:

Proposition 4.8. *For any thin cycle $\gamma_k \in \mathcal{G}_f$, one can compute a (not necessarily thin) cycle $\widehat{\gamma_k}$ such that $\gamma_k = \text{dom}(\widehat{\gamma_k})$ and*

$$\phi(\widehat{\gamma_k}) \in \sum_{j=1}^{r} \zeta_{k_j} + Z_1^{2\delta}(R_g),$$

where each $\zeta_{k_j} \in \mathcal{G}_g$ is 3δ-close to γ_k, for any $j \in [1, r]$.

Proof. Assume that the thin basis decomposition of $\phi(\gamma_k)$ has the form:

$$\phi(\gamma_k) \in \sum_{j=1}^{r} \zeta_{k_j} + \sum_{j=1}^{s} \tilde{\zeta}_j + Z_1^{2\delta}(R_g),$$

11

where the first term contains the 2δ-stable thin cycles whose range is 3δ-Hausdorff close to range(γ_k), the last term contains the thin cycles that are not 2δ-stable, and the middle term contains those thin cycles $\tilde{\zeta}_j$ that are neither 3δ-close to γ_k nor small. We wish to get rid of the middle term $\tilde{\zeta} = \sum_{j=1}^{s} \tilde{\zeta}_j$. Set $\gamma' = \psi(\tilde{\zeta})$. By Lemma 4.5, we have that $\phi(\gamma') = \phi \circ \psi(\tilde{\zeta}) \in \tilde{\zeta} + Z_1^{2\delta}(R_g)$. Set $\widehat{\gamma}_k := \gamma_k + \gamma'$. It is then easy to verify that $\phi(\widehat{\gamma}_k) = \phi(\gamma_k) + \phi(\gamma') \in \sum_{j=1}^{r} \zeta_{k_j} + Z_1^{2\delta}(R_g)$, as claimed.

It remains to show that dom($\widehat{\gamma}_k$) = γ_k. Let $[b,d]$ = range(γ_k). By Lemma 4.6, range($\tilde{\zeta}_j$) $\subseteq [b - \delta, d + \delta]$, for any $j \in [1, s]$. Since each $\tilde{\zeta}_j$ is not 3δ-close to γ_k, it is then necessary that, for any $j \in [1, s]$, either range($\tilde{\zeta}_j$) $\subseteq [b - \delta, d - 3\delta)$ or range($\tilde{\zeta}_j$) $\subseteq (b + 3\delta, d + \delta]$. W.l.o.g. assume that range($\tilde{\zeta}_j$) $\subseteq [b - \delta, d - 3\delta)$. Apply Lemma 4.6 to the cycle $\tilde{\zeta}_j$. We have that the range of any cycle in the thin basis decomposition of $\psi(\tilde{\zeta}_j)$ is contained in $[b - 2\delta, d - 2\delta)$, thus its height strictly smaller than $d - b$. Hence all cycles in the thin basis decomposition of $\gamma' = \psi(\tilde{\zeta})$ have a height strictly smaller than height(γ_k) = $d - b$. This means that γ_k has the largest height among the cycles of the thin basis decomposition of $\widehat{\gamma}_k = \gamma_k + \gamma'$, and it is the only cycles with this largest height. It then follows that $\gamma_k = $ dom($\widehat{\gamma}_k$). $\qquad\square$

Corollary 4.9. *Let $\widehat{\mathcal{G}}_f$ denote the set of cycles $\{\widehat{\gamma}_k\}_{k=1}^{n}$, where each $\widehat{\gamma}_k$ is as specified in Proposition 4.8. $\widehat{\mathcal{G}}_f$ forms a basis for $Z_1(R_f)$.*

Proof. Since the dominating cycles for cycles in $\widehat{\mathcal{G}}_f$ are all distinct, it follows from Lemma 4.4 that all cycles in $\widehat{\mathcal{G}}_f$ are linearly independent. Hence $\widehat{\mathcal{G}}_f$ also forms a (not necessarily thin) basis for $Z_1(R_f)$. $\qquad\square$

Let Φ denote the matrix of the mapping from the base cycles in $\widehat{\mathcal{G}}_f$ (columns, domain) to those in $\mathcal{G}_g$ (rows, range) as induced by ϕ, i.e., the ith column of Φ specifies the representation of $\phi(\widehat{\gamma}_i)$ using basis elements from $\mathcal{G}_g$, with $\Phi_{ij} = 1$ if ζ_j is in the thin basis decomposition of $\phi(\widehat{\gamma}_i)$. Let $\widetilde{\Phi}$ be the submatrix of Φ with columns corresponding to basis elements $\widehat{\gamma}_i$ that are 3δ-stable, and rows corresponding to basis elements ζ_j that are 2δ-stable. See Fig. 2 (a). By Proposition 4.8, $\widetilde{\Phi}_{ij} = 1$ implies that the basis element $\zeta_j \in \mathcal{G}_g$ is 3δ-close to the basis element $\gamma_i \in \mathcal{G}_f$. Recall that our goal is to show that there is a 3δ-matching for $\mathcal{G}_f$ and $\mathcal{G}_g$. Intuitively, non-zero entries in $\widetilde{\Phi}$ will provide potential matchings for basis elements in $\mathcal{G}_f$ to establish a 3δ-matching between $\mathcal{G}_f$ and $\mathcal{G}_g$ that we need.

Lemma 4.10. *The columns of $\widetilde{\Phi}$ are linearly independent.*

Proof. Consider an arbitrary subset of indices $i_1, \ldots, i_s$ whose corresponding columns are in $\widetilde{\Phi}$ (i.e, each $\widehat{\gamma}_{i_a}$ is 3δ-stable), and let $\widehat{\gamma} = \widehat{\gamma}_{i_1} + \cdots + \widehat{\gamma}_{i_s}$. We will show that $\phi(\widehat{\gamma})$ is 2δ-stable; that is, dom($\phi(\widehat{\gamma})$) has height at least 4δ. This means that the linear combination of the corresponding columns in $\widetilde{\Phi}$ contains a non-zero element. Since this holds for any subset of columns from $\widetilde{\Phi}$, we have that the columns in $\widetilde{\Phi}$ are linearly independent.

It remains to show that $\phi(\widehat{\gamma})$ is 2δ-stable. Recall that for any index a, γ_a is the dominating cycle of $\widehat{\gamma}_a$. Assume w.l.o.g. that γ_{i_1} has the largest height among all γ_{i_j}, for $j \in [1, s]$. (If there are multiple cycles from $\{\gamma_{i_j}\}_{j=1}^{s}$ having this largest height, let γ_{i_1} be the one with smallest index.) From the end of the proof of Proposition 4.8, we note that for any index a, γ_a is the *only* cycle with maximum height among all cycles in the thin basis decomposition of $\widehat{\gamma}_a$. In other words, all other cycles in the thin basis decomposition of $\widehat{\gamma}_a$ have strictly smaller height than γ_a. Putting these together, it follows that γ_{i_1} must exist in the thin basis decomposition of $\widehat{\gamma}$ w.r.t. the original thinnest basis $\mathcal{G}_f$ and in fact, $\gamma_{i_1} = $ dom($\widehat{\gamma}$). Since γ_{i_1} is 3δ-stable (thus its height at least 6δ), it then follows from Lemma 4.7 that height(dom($\phi(\widehat{\gamma})$)) $\geq$ height(dom($\widehat{\gamma}$)) $- 2\delta > 4\delta$. So $\phi(\widehat{\gamma})$ is 2δ-stable. $\qquad\square$

Corollary 4.11. *We can identify a unique row index i for each column index j in $\widetilde{\Phi}$ such that $\widetilde{\Phi}_{ij} = 1$.*
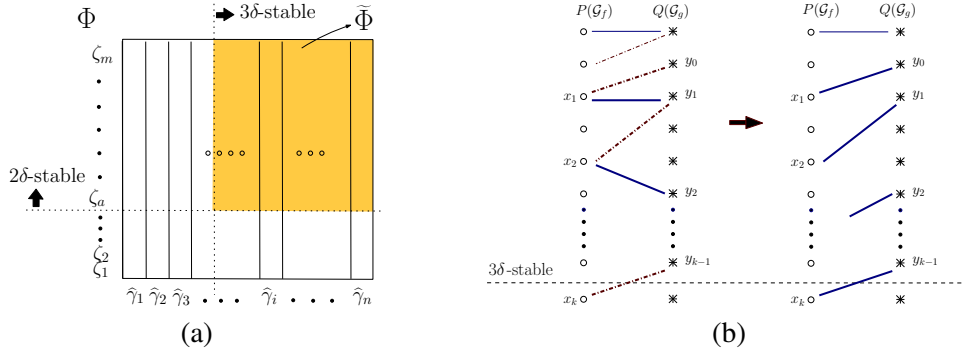
12

Figure 2: (a): The ith column in the matrix Φ specifies the representation of $\phi(\widehat{\gamma_i})$ using the basis elements in $\mathcal{G}_g$. The shaded submatrix represents $\widetilde{\Phi}$. (b): A bipartite graph view of the augmenting process. Left: Thick path alternates between an F-induced (solid) and an G-induced (dash-dotted) edge. Right: Thick solid edges are induced by the modified injective map $\widehat{F}$ (which are used to be G-induced edges in the left figure).

Proof. View the matrix $\widetilde{\Phi}$ as the adjacency matrix for the following bipartite graph $G = (P \cup Q, E)$, where P are the columns of $\widetilde{\Phi}$, Q are the rows, and there is an edge between $p \in P$ and $q \in Q$ iff the corresponding entry in the matrix $\widetilde{\Phi}$ is 1. We now claim that there is a *P-saturated matching* for G: that is, there is a matching of G such that every node in P is matched exactly once, and each node in Q is matched at most once. Note that this immediately implies the claim. Specifically, for any subset of nodes $P' \subseteq P$, let $Q' \subseteq Q$ be the union of neighbors of nodes from P'. In other words, Q' is the set of rows with at least one non-zero entry in the columns P'. If $|Q'| < |P'|$, then these columns of $\widetilde{\Phi}$ will be linearly dependent, which violates Lemma 4.10. Hence we have $|Q'| \geq |P'|$. Now by Hall's Theorem (see, e.g., Page 35 of [36]), a P-satuated matching exists for G. $\square$

Proof of Theorem 4.3. Recall that by Proposition 4.8, $\widetilde{\Phi}_{ij} = 1$ implies that the cycles γ_j and ζ_i are 3δ-close. It follows from Corollary 4.11 that there is an injective map F from the set of 3δ-stable cycles in $\mathcal{G}_f$ to the cycles in $\mathcal{G}_g$ such that each pair of corresponding cycles are 3δ-close. By a symmetric argument (switching the role of R_f and R_g), there is also an injective map G from the 3δ-stable cycles in $\mathcal{G}_g$ to cycles in $\mathcal{G}_f$ where each corresponding pair of cycles are 3δ-close. However, F and G may not be consistent and do not directly give rise to a 3δ-matching of $\mathcal{G}_f$ and $\mathcal{G}_g$ yet. In what follows, we will modify F to obtain another *injective* map $\widehat{F}$ such that (i) any 3δ-stable cycle in $\mathcal{G}_f$ is mapped by $\widehat{F}$ to a cycle in $\mathcal{G}_g$ that is 3δ-close, and (ii) all 3δ-stable cycles in $\mathcal{G}_g$ are contained in im $\widehat{F}$, the image of $\widehat{F}$. Note that $\widehat{F}$ provides exactly the set of correspondences necessary in a 3δ-matching between $\mathcal{G}_f$ and $\mathcal{G}_g$. In particular, the injectivity of $\widehat{F}$ and these conditions guarantee that the condition (II) of a 3δ-matching. As discussed at the beginning of this section, this then means that $d_B(\mathrm{ExDg}_1(R_f), \mathrm{ExDg}_1(R_g)) \leq 3\delta = 3d_{FD}(R_f, R_g)$, proving Theorem 4.3.

It remains to show how to construct $\widehat{F}$ satisfying conditions (i) and (ii) above. Conditions (i) already holds for F, so the main task is to establish condition (ii) while maintaining (i). Start with $\widehat{F} = F$. Let $y_0 \notin$ im $\widehat{F}$ be any 3δ-stable cycle in $\mathcal{G}_g$ that is not yet in im $\widehat{F}$. Let $x_1 = G(y_0) \in \mathcal{G}_f$. We continue with $y_i = \widehat{F}(x_i)$ if x_i is 3δ-stable. Next, if y_i is 3δ-stable, then set $x_{i+1} = G(y_i)$. We repeat this process, until we reach x_k or y_k which is not 3δ-stable any more. At this time, we modify $\widehat{F}(x_i)$ to be y_{i-1} for each $j \in [1, k]$ (originally, $\widehat{F}(x_i) = y_i$). Throughout this process, all y_i other than y_0 are already in im $\widehat{F}$. After the modification of $\widehat{F}$, we have $y_0 \in$ im $\widehat{F}$, while all other y_i remain in im $\widehat{F}$. The only exception is when the above process terminates by reaching some y_k which is not 3δ-stable (the termination condition), in which case y_k will not be in im $\widehat{F}$ after the modification of $\widehat{F}$. However, the number of 3δ-stable cycles contained in im $\widehat{F}$ increases by one (i.e., y_0) by the above process. It is easy to verify that since F is injective, $\widehat{F}$ remains injective. Furthermore, x_i and $y_{i-1} = \widehat{F}(x_i)$ are still 3δ-close, since by construction $x_i = G(y_{i-1})$.

13

An alternative way to view this is to consider the specific bipartite graph $G' = (P \cup Q, E')$, where nodes in P and Q correspond to basis cycles in $\mathcal{G}_f$ and $\mathcal{G}_g$, respectively, and edges E' are those corresponding to a cycle and its image under either the map $\widehat{F}$ or G. The sequence $y_0, x_1, y_1, \ldots$ specifies a path with edges alternating between the $\widehat{F}$-induced and the G-induced matchings. The modified assignment of $\widehat{F}(x_j)$ changes a G-induced matching to an $\widehat{F}$-induced matching along this path, much similar to the use of augmenting paths to obtain maximum bipartite matching. See Fig. 2 (b) for an illustration.

We repeat the above path augmentation process for any remaining 3δ-stable cycle in $\mathcal{G}_g \setminus \text{im } \widehat{F}$. This process will terminate because after each augmentation process, the number of 3δ-stable cycles contained in im $\widehat{F}$ strictly increases. In the end, we obtain an injective map $\widehat{F}$ from the set of 3δ-stable cycles of $\mathcal{G}_f$ to cycles in $\mathcal{G}_g$ such that im $\widehat{F}$ contains all 3δ-stable cycles of $\mathcal{G}_g$. Hence, $\widehat{F}$ induces a 3δ-matching from $\text{ExDg}_1(R_f)$ to $\text{ExDg}_1(R_g)$, finishing the proof of Theorem 4.3.

5   Relation to Gromov–Hausdorff Distance

As mentioned earlier in Section 3, the functional distortion distance can be considered as a variant of the Gromov-Hausdorff distance (between metric spaces), restricted to continuous correspondences and taking function values into account. We now discuss this relation in more detail.

We can view the Reeb graphs R_f and R_g as metric spaces, equipped with metrics d_f and d_g, respectively. A natural distance for metric spaces is the *Gromov–Hausdorff* distance, which, using the notation of Eq. (4), is defined as

$$d_{GH}(R_f, R_g) = \inf_{\phi, \psi} \left(D(\phi, \psi) \right), \tag{7}$$

where $\phi : R_f \to R_g$ and $\psi : R_g \to R_f$ range over all maps between R_f and R_g. Here the maps ϕ, ψ are not required to be continuous, which is different from our definition of the functional distortion distance.

Note that translation $f + c$ and negation $-f$ do not change the metric structures of the Reeb graph R_f. To account for the difference in function values, we define the *functional GH distance* between R_f and R_g, which measures not only the metric distortion but also the difference in function values between corresponding points:

$$d_{fGH}(R_f, R_g) := \inf_{\phi, \psi} \max \left(D(\phi, \psi), \|f - g \circ \psi\|_\infty, \|f \circ \phi - g\|_\infty \right), \tag{8}$$

where ϕ and ψ range over all maps between R_f and R_g.

It turns out that we have the following relations, which imply that the functional distortion distance roughly measures the minimum distortion in both function values (between f and g) and in their induced metrics (between d_f to d_g).

Theorem 5.1. $d_{fGH}(R_f, R_g) \le d_{FD}(R_f, R_g) \le 3d_{fGH}(R_f, R_g)$.

We note that a similar result also holds for the Gromov–Hausdorff distance, without the terms controlling the function values. Specifically, for metrics d_f and d_g the standard Gromov–Hausdorff distance as defined in Eq. (7) is equivalent to its continuous variant up to a constant factor, restricting ϕ and ψ to continuous maps. This relation does not hold in general.

Proof. The left inequality $d_{fGH}(R_f, R_g) \le d_{FD}(R_f, R_g)$ is immediate from the definitions. We now prove the right inequality $d_{FD}(R_f, R_g) \le 3d_{fGH}(R_f, R_g)$. Fix an arbitrary positive real value ε. Let C denote an *ε-optimal correspondence*, i.e., the maximum of the three terms in the right hand side of Eq. (8) is less than or equal to $d_{fGH}(R_f, R_g) + \varepsilon$. Set $\beta = d_{fGH}(R_f, R_g)$. Our final goal is to show that $d_{FD}(R_f, R_g) \le 3\beta$. We do this

by constructing *continuous* maps $\phi^\varepsilon : R_f \to R_g$ and $\psi^\varepsilon : R_g \to R_f$, based on the ε-optimal pair of maps (ϕ, ψ) (which are not necessarily continuous), so that each of the terms in Eq. (5) can be bounded by $3\beta + O(\varepsilon)$.

We now show how to construct a certain *continuous* map $\phi^\varepsilon : R_f \to R_g$ from the map $\phi : R_f \to R_g$. To do so, we will first construct an *ε-subdivition of R_f* as follows: We subdivide all arcs in R_f to obtain a set of nodes $V_\varepsilon = \{v_1, \ldots, v_N\}$ such that f is monotonic on each resulting arc, and the height of an arc $v_i v_j$ (which is $|f(v_i) - f(v_j)|$ since f is monotonic on $v_i v_j$) is at most ε. We set $\phi^\varepsilon(v_i) = \phi(v_i)$.

Next, we extend this map defined on the nodes in V_ε to a continuous map defined on the entire graph R_f. In particular, consider an arc $v_i v_j$ and assume w.l.o.g. that $f(v_i) \le f(v_j)$. Consider $\tilde{v}_i = \phi^\varepsilon(v_i)$ and $\tilde{v}_j = \phi^\varepsilon(v_j)$. Since (ϕ, ψ) is ε-optimal, we know that

$$\frac{1}{2}|d_f(v_i, v_j) - d_g(\tilde{v}_i, \tilde{v}_j)| \le \beta + \varepsilon,$$

thus

$$d_g(\tilde{v}_i, \tilde{v}_j) \le d_f(v_i, v_j) + 2(\beta + \varepsilon) \le 2\beta + 3\varepsilon.$$

This means that there is an embedded path $\pi(\tilde{v}_i, \tilde{v}_j)$ in R_g connecting $\tilde{v}_i$ to $\tilde{v}_j$ whose height is at most $2\beta + 3\varepsilon$. We now extend ϕ^ε to an arbitrary homeomorphism from the arc $v_i v_j$ of R_f to this path $\pi(\tilde{v}_i, \tilde{v}_j)$ with $\phi^\varepsilon(v_i) = \tilde{v}_i$ and $\phi^\varepsilon(v_j) = \tilde{v}_j$. Assembling all these pieces of ϕ^ε on each arc of R_f yields the continuous map $\phi^\varepsilon : R_f \to R_g$.

Given any point $x \in R_f$, assume that x lies on the arc $v_i v_j$. Then $\tilde{x} := \phi^\varepsilon(x)$ is mapped to some point in $\pi(\tilde{v}_i, \tilde{v}_j)$. Since (ϕ, ψ) is ε-optimal, by definition in Eq. (8),

$$g(\tilde{v}_i) \in [f(v_i) - \beta - \varepsilon, f(v_i) + \beta + \varepsilon] \quad \text{and} \quad g(\tilde{v}_j) \in [f(v_j) - \beta - \varepsilon, f(v_j) + \beta + \varepsilon].$$

Since the path $\pi(\tilde{v}_i, \tilde{v}_j)$ has height at most $2\beta + 3\varepsilon$, we then have

$$\text{range}(\pi(\tilde{v}_i, \tilde{v}_j)) \in [f(v_i) - 3\beta - 4\varepsilon, f(v_j) + 3\beta + 4\varepsilon].$$

Since $x \in v_i v_j$ and $\tilde{x} \in \pi(\tilde{v}_i, \tilde{v}_j)$, it then follows that $g(\tilde{x}) \in [f(v_i) - 3\beta - 4\varepsilon, f(v_j) + 3\beta + 4\varepsilon]$ and thus $|g(\tilde{x}) - f(x)| \le 3\beta + 5\varepsilon$ for any $x \in R_f$. Hence we have that $\max_{x \in R_f} |f(x) - g \circ \phi^\varepsilon(x)| \le 3\beta + 5\varepsilon$.

Symmetrically, we can take an ε-subdivision of R_g with nodes $U_\varepsilon = \{\tilde{u}_1, \ldots, \tilde{u}_M\}$, and construct a continuous map $\psi^\varepsilon : R_g \to R_f$. Using the same argument as above, we have that $\max_{\tilde{y} \in R_g} |g(\tilde{y}) - f(\psi^\varepsilon(\tilde{y}))| \le 3\beta + 5\varepsilon$.

We now bound $d_f(x, y) - d_g(\tilde{x}, \tilde{y})$ for any $(x, \tilde{x}), (y, \tilde{y}) \in G(\phi^\varepsilon, \psi^\varepsilon)$. If $x \in v_i v_j$ and $\tilde{x} \in \pi(\tilde{v}_i, \tilde{v}_j)$ (i.e, $\tilde{x} = \phi^\varepsilon(x)$), we let $w_i = v_i$ and $\tilde{w}_i = \tilde{v}_i$ and have $d_f(x, w_i) \le \varepsilon$ and $d_g(\tilde{x}, \tilde{w}_i) \le 2\beta + 3\varepsilon$ (as the height of path $\pi(\tilde{v}_i, \tilde{v}_j)$ is at most $2\beta + 3\varepsilon$ as discussed earlier). If, on the other hand, $\tilde{x} \in \tilde{u}_i \tilde{u}_j$ and $x \in \pi(u_i, u_j)$ (i.e, $x = \psi^\varepsilon(\tilde{x})$), we let $w_i = u_i$ and $\tilde{w}_i = \tilde{u}_i$ and have $d_f(x, w_i) \le 2\beta + 3\varepsilon$ and $d_g(\tilde{x}, \tilde{w}_i) \le \varepsilon$. In either case, we have $d_f(x, w_i) + d_g(\tilde{x}, \tilde{w}_i) \le 2\beta + 4\varepsilon$. See the illustrations of both cases below. In an analogous way, we also obtain

$w_a, \tilde{w}_a$ with $d_f(y, w_a) + d_g(\tilde{y}, \tilde{w}_a) \le 2\beta + 4\varepsilon$. Note that by the construction of ϕ^ε and ψ^ε, both $(w_i, \tilde{w}_i)$ and $(w_a, \tilde{w}_a)$ are from the ε-optimal correspondence generated by the maps (ϕ, ψ). In other words, we have that $d_f(w_i, w_a) \le d_g(\tilde{w}_i, \tilde{w}_a) + 2\beta + 2\varepsilon$. It then follows that:

$$\begin{aligned}
d_f(x, y) &\le d_f(x, w_i) + d_f(w_i, w_a) + d_f(w_a, y) \\
&\le d_f(x, w_i) + d_f(w_a, y) + (d_g(\tilde{w}_i, \tilde{w}_a) + 2\beta + 2\varepsilon) \\
&\le d_f(x, w_i) + d_f(w_a, y) + 2\beta + 2\varepsilon + d_g(\tilde{w}_i, \tilde{x}) + d_g(\tilde{x}, \tilde{y}) + d_g(\tilde{y}, \tilde{w}_a) \\
&\le d_g(\tilde{x}, \tilde{y}) + 6\beta + 10\varepsilon.
\end{aligned}$$

By symmetry of the above argument, we obtain

$$\frac{1}{2}\left|d_f(x,\tilde{x}) - d_g(y,\tilde{y})\right| \le 3\beta + 5\varepsilon.$$

Putting everything together, we have that $d_{FD}(R_f, R_g) \le \lim_{\varepsilon \to 0} 3\beta + 5\varepsilon = 3d_{fGH}(R_f, R_g)$. $\qquad\square$

6 Relation to Interleaving Distance for Merge Trees

A merge tree is simply a rooted tree T_f equipped with a function $f : T_f \to \mathbb{R}$ such that the function value of f from the root to any leaf is monotonically descreasing. For technical reasons, the version of "merge trees" defined by Morozov et al. [16] further adds an extra arc from the root whose function value extends to $+\infty$, and they proposed an *interleaving distance* for two merge trees under this modification. From now on, we assume merges are such extended merge trees.

We first introduce the interleaving distance for merge trees defined in [16]. Assume that we are given two merge trees T_f and T_g with associated functions $f : T_f \to \mathbb{R}$ and $g : T_g \to \mathbb{R}$.

Definition 6.1 ([16])**.** *Two continuous maps* $\alpha^\varepsilon : T_f \to T_g$ *and* $\beta^\varepsilon : T_g \to T_f$ *are said to be* ε-compatible *for some* $\varepsilon \ge 0$, *if*

$$g(\alpha^\varepsilon(x)) = f(x) + \varepsilon\,; \qquad\qquad f(\beta^\varepsilon(y)) = g(y) + \varepsilon; \qquad\qquad (9)$$
$$\beta^\varepsilon \circ \alpha^\varepsilon = \mathrm{i}^{2\varepsilon}\,; \qquad\qquad \alpha^\varepsilon \circ \beta^\varepsilon = \mathrm{j}^{2\varepsilon}; \qquad\qquad (10)$$

where $\mathrm{i}^{2\varepsilon} : T_f \to T_f$ *and* $\mathrm{j}^{2\varepsilon} : T_g \to T_g$ *are the* 2ε-shift maps in the respective trees.

The interleaving distance, $d_I(T_f, T_g)$, *between two merge trees* T_f *and* T_g, *is the greatest lower bound on* ε *for which there are* ε-compatible maps:

$$d_I(T_f, T_g) = \inf\{\varepsilon \mid \text{ there are } \varepsilon \text{ compatible maps } \alpha^\varepsilon : T_f \to T_g \text{ and } \beta^\varepsilon : T_g \to T_f\}. \qquad (11)$$

Let $d_{FD}(T_f, T_g)$ be the functional distortion distance for Reeb graphs that we introduced. The main result of this section is that, for merge trees, the interleaving distance of [16] and our functional distortion distance are isometric.

Theorem 6.2. *Given two merge trees* T_f *and* T_g, *equipped with functions* $: T_f \to \mathbb{R}$ *and* $g : T_g \to \mathbb{R}$, *we have* $d_I(T_f, T_g) = d_{FD}(T_f, T_g)$.

Proof. We break down the proof into two steps, which are shown in Lemmas 6.3 and 6.4. $\qquad\square$

Lemma 6.3. $d_{fGH}(T_f, T_g) \le d_I(T_f, T_g)$.

Proof. Let $\varepsilon = d_I(T_f, T_g)$. We assume that ε is obtained by a pair of ε-compatible maps[3], $\alpha^\varepsilon : T_f \to T_g$ and $\beta^\varepsilon : T_g \to T_f$. We will show that the correspondances generated by these two maps α^ε and β^ε induce a distance distortion at most ε. This implies that $d_{FD}(T_f, T_g) \le \varepsilon$. Specifically, let $G(\alpha^\varepsilon, \beta^\varepsilon)$ and $D(\alpha^\varepsilon, \beta^\varepsilon)$ as introduced in Eq. (4). We now bound $D(\alpha^\varepsilon, \beta^\varepsilon)$.

Consider two pairs $(x_1, y_1), (x_2, y_2) \in G(\alpha^\varepsilon, \beta^\varepsilon)$. we first aim to bound $|d_f(x_1, x_2) - d_g(y_1, y_2)|$ from above.

Assume first that $y_1 = \alpha^\varepsilon(x_1)$ and $y_2 = \alpha^\varepsilon(x_2)$. Let π_1 be the optimal path connecting x_1 to x_2 that achieves $d_f(x_1, x_2)$, which is necessarily the unique simple path connecting x_1 to x_2 in the tree T_f. Its image $\pi_1' = \alpha^\varepsilon(\pi_1)$ is a path connecting y_1 and y_2. By Eq. (9), α^ε shift every point up by ε in the corresponding

---

[3]We note that ε may be only achieved in the limit. Our argument can be extended to that case by taking a sequence of ε'-compatible maps and send ε' to ε.

function value. Hence the range of π_1 is shifted up by ε to the range of π_1' while their heights are the same. Hence we have $d_g(y_1, y_2) \le d_f(x_1, x_2)$.

Now consider the optimal path π_2 connecting y_1 to y_2 to achieve $d_g(y_1, y_2)$ in T_g. Let $x_1' = \beta^\varepsilon(y_1)$, $x_2' = \beta^\varepsilon(y_2)$. The image $\pi_2' = \beta^\varepsilon(\pi_2)$ of π_2 under the map β^ε is a path connecting x_1' to x_2' in T_f. Similarly, we have that height(π_2) = height(π_2') and the range of π_2 is translated up by ε to π_2'. On the other hand, by Eq. (10), we have $x_1' = \mathrm{i}^{2\varepsilon}(x_1)$, and $x_2' = \mathrm{i}^{2\varepsilon}(x_2)$. By the definition of the shift map, there is a monotone path from x_1 to x_1' (along the path from x_1 to the root of the merge tree T_f) in T_f; and similarly for x_2 and x_2'. Concatenating these two montone paths with π_2' we obtain a path π_3 connecting x_1 to x_2. Since the two new paths are monotone, of height 2ε each, and both going up, we have that height$(\pi_3) \le$ height$(\pi_2') + 2\varepsilon =$ height$(\pi_2) + 2\varepsilon$. It then follos that $d_f(x_1, x_2) \le d_g(y_1, y_2) + 2\varepsilon$. Putting this together with that $d_g(y_1, y_2) \le d_f(x_1, x_2)$ proved earlier, we thus have $|d_f(x_1, x_2) - d_g(y_1, y_2)| \le 2\varepsilon$.

If the two pairs are obtained via $x_1 = \beta^\varepsilon(y_1)$ and $x_2 = \beta^\varepsilon(y_2)$, a symmetric argument will show $|d_f(x_1, x_2) - d_g(y_1, y_2)| \le 2\varepsilon$ as well.

We now consider the remaining case where $y_1 = \alpha^\varepsilon(x_1)$ but $x_2 = \beta^\varepsilon(y_2)$. Let π be the optimal path connecting x_1 to x_2 in T_f to achieve $d_f(x_1, x_2)$. Let $\pi' = \beta^\varepsilon(\pi)$ be its image in T_g: note π' connects y_1 to $y_2' = \beta^\varepsilon(x_2)$. By Eq. (9) of the definition of ε-compatible maps, we have that π' is of the same height of π (and its range is that of π shifted upward by ε). By Eq. (10) of the definition of ε-compatible maps, we have that $y_2' = \mathrm{j}^{2\varepsilon}(y_2)$ and thus there is a monotone path π_4 of height 2ε connecting y_2 to y_2'. Hence the concatenation $\pi_5 = \pi' \circ \pi_4$ is a path connecting y_1 to y_2. Thus height$(\pi_5) \le$ height$(\pi') + 2\varepsilon =$ height$(\pi) + 2\varepsilon$, implying that $d_g(y_1, y_2) \le d_f(x_1, x_2) + 2\varepsilon$.

A symmetric argument shows that $d_f(x_1, x_2) \le d_g(y_1, y_2) + 2\varepsilon$. Hence $|d_f(x_1, x_2) - d_g(y_1, y_2)| \le 2\varepsilon$. It then follows that $D(\alpha^\varepsilon, \beta^\varepsilon) \le \varepsilon$. On the other hand, by Eq. (9), $\|f - g \circ \alpha^\varepsilon\|_\infty = \varepsilon$ and $\|f \circ \phi_\leftarrow - g\|_\infty = \varepsilon$. By Eq. (5), it then follows that $d_{FD}(T_f, T_g) \le \varepsilon$. $\qquad \square$

Lemma 6.4. $d_I(T_f, T_g) \le d_{FD}(T_f, T_g)$.

Proof. Let $\delta = d_{FD}(T_f, T_g)$ denote the functional distortion-distance between two merge trees T_f and T_g, and let $\phi^* : T_f \to T_g$ and $\psi^* : T_g \to T_f$ be the optimal continuous maps[4] achieving δ. We will now construct a pair of δ-compatible maps for T_f and T_g using ϕ^* and ψ^*. This then implies that $d_I(T_f, T_g) \le d_{FD}(T_f, T_g)$ as claimed.

First, we construct the map $\alpha^\delta : T_f \to T_g$ as follows: For every point $x \in T_f$, let $y = \phi^*(x)$. Now set $\rho = f(x) + \delta - g \circ \phi^*(x)$ — by the definition of d_{FD} in Eq. (5), ρ is a non-negative real value in the range $[0, 2\delta]$. We now set $\alpha^\delta(x) = \mathrm{j}^\rho(y) = \mathrm{j}^\rho \circ \phi^*(x)$. Easy to see that by the choice of ρ, $g(\alpha^\delta(x)) = f(x) + \varepsilon$. Since ϕ^* is continuous, the function $\rho : T_f \to \mathbb{R}$ is continuous, and the map α^δ is thus also a continuous map. Similarly, we construct $\beta^\delta : T_g \to T_f$. By their construction, the requirements in Eq. (9) are satisfied. We now show that Eq. (10) also hold for α^δ and β^δ.

Indeed, consider a point $x \in T_f$, and let $y = \phi^*(x)$ and $y' = \alpha^\delta(x)$. By the definitino of α^δ, $g(y') = f(x) + \delta \ge g(y)$ and there is a monotone path π connecting y to y' (in particular, y' is along the path from y to the root of the merge tree T_g). Now map π back to T_f via the map β^δ, which is necessarily a monotone path π' connecting $\tilde{x} := \beta^\delta(y)$ and $x' := \beta^\delta(y') = \beta^\delta \circ \alpha^\delta(x)$. In other words, x' is along the path from $\tilde{x}$ to the root of the merge tree T_f. By the definition of α^δ and β^δ, $f(x') = f(x) + 2\delta$. We now show that x' is along the path from x to the root of the merge tree T_f: this would then imply that $x' = \mathrm{i}^{2\delta}$, namely, $\beta^\delta \circ \alpha^\delta = \mathrm{i}^{2\delta}$.

To see that there is a monotone path from x up to x' in T_f, set $\tilde{x}' = \psi^*(y)$. By the construction of β^δ, $\tilde{x}$ is along the unique monotone path from $\tilde{x}'$ up to the root of T_f. Furthermore, $f(\tilde{x}) = g(y) + \delta$, $f(\tilde{x}') \in [g(y) - \delta, g(y) + \delta]$ and $f(\tilde{x}') \le f(\tilde{x})$. Note that (x, y) and $(\tilde{x}', y)$ are in the set of correspondances $\mathcal{G}(\phi^*, \psi^*)$ (this is because $y = \phi^*(x)$ and $\tilde{x}' = \psi^*(y)$). Hence by the definition of d_{FD} which is achieved by ϕ^* and ψ^*,

---

[4]Again, if the optimal is achieved in the limit, we can modify our argument by taking a sequence of near optimal maps and take them to the limit.

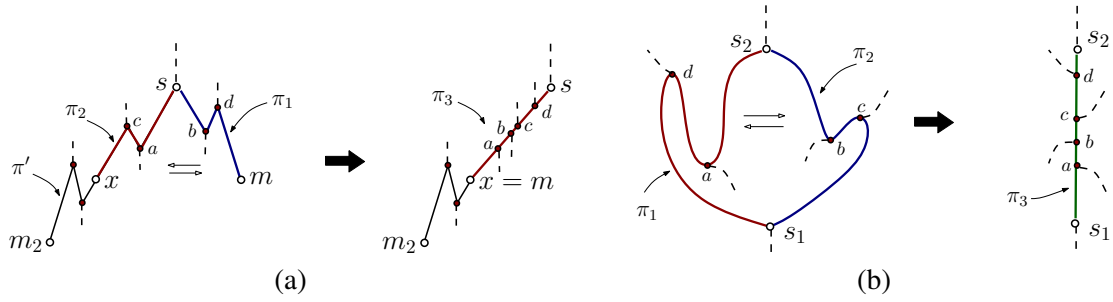Figure 3: (a): Removing a branching feature spanned by (m, s) by merging paths π_1 and π_2. This removes the point $(f(m), f(s))$ from the 0-th ordinary persistence diagram. (b): Removing a cycle feature spanned by (s_1, s_2); this removes the point $(f(s_1), f(s_2))$ from the 1st extended persistence diagram.

there is a path $\tilde{\pi}$ connecting x to $\tilde{x}'$ such that $\mathrm{height}(\tilde{\pi}) \leq 2\delta$. This means that the least common ancester of x and $\tilde{x}'$ has a function value at most $f(x) + 2\delta$ which is $f(x')$. Since $\tilde{x}'$ and $\tilde{x}$ are connected by a monotone path, the least common ancester of x and $\tilde{x}$ has a function value at most $f(x')$. Since x' is an ancester of $\tilde{x}$, it follows that x' is an ancestor for x as well. Hence $x' = i^{2\delta}(x)$ and $\beta^\delta \circ \alpha^\delta = i^{2\delta}$. A symmetric argument shows that $\alpha^\delta \circ \beta^\delta = i^{2\delta}$. Putting everything together, we have that α^δ and β^δ form a δ-compatible pair of maps between T_f and T_g. As such, $d_I(T_f, T_g) \leq \delta = d_{FD}(T_f, T_g)$.

□

7 Simplification of Reeb Graphs

Reeb graphs have been used as a meaningful summary of the input functions. Simplifying a Reeb graph can help to remove noise or single out major features, and to create a multi-resolution representation of the input domain; see e.g., [19, 22, 31]. As we described in Section 2, there is a natural way to quantify branching and loop features in terms of ordinary and extended persistence in the according dimensions. Indeed, it is common practice to simplify the Reeb graph by removing all features with persistence smaller than a given threshold. In this section, we prove that by removing small features using a natural merging strategy, (branching and loop) features with large persistence will not be killed, and will roughly maintain their persistence ("importance").

7.1 A Natural Simplification Scheme for Reeb Graphs

We first introduce a natural simplification scheme for Reeb graphs (see, e.g., [22, 31]). See Fig. 3 for an illustration.

Given an ordinary persistence pair (m, s), assume that m is a minimum and s is a down-fork. Recall that the down-fork s merges two connected components C_1 and C_2 of the sublevel set below $f(s)$, and m is the higher minimum of the two. To remove the feature (m, s), we wish to merge the branch containing m, say C_1, into the other branch C_2, so that afterwards, m and s become regular points (i.e., with up-degree and down-degree both being 1). In particular, we perform the following operation (see Fig. 3 (a)). Let m_2 denote the minimum of C_2. We choose an arbitrary embedded path $\pi_1 \subseteq C_1$ from s to m, and an arbitrary $\pi' \subseteq C_2$ from s to m_2. Now imagine we traverse π' starting from s. We stop when we encounter the first point x on π' such that $f(x) = f(m)$, and set π_2 to be the subcurve of π' from s to x. By identifying points with the same function value, we merge $\mathrm{im}\,\pi_1$ and $\mathrm{im}\,\pi_2$ to form the image of a new monotonic arc π_3 between s and x such that any point $p \in \mathrm{im}\,\pi_1 \cup \mathrm{im}\,\pi_2$ is mapped to some $q \in \mathrm{im}\,\pi_3$ with $f(q) = f(p)$. Pairs of type (up-fork, maximum) are treated in a symmetric way.

18

Given an extended persistence pair (s_1, s_2) between an up-fork s_1 and a down-fork s_2, let γ be a thin cycle that spans it. W.l.o.g. assume that $\text{im}\,\gamma$ consists only of a single connected component: if $\text{im}\,\gamma$ has multiple connected components, then there must exist one that contains both s_1 and s_2. That component is necessarily an embedded loop and thus we can simply set γ to be the thin cycle corresponding to that loop. Let π_1 and π_2 denote the two disjoint sub-curves of the loop that connect s_1 and s_2. To cancel the feature, intuitively, we wish to merge π_1 and π_2 to kill the cycle γ. Note that π_1 and π_2 may not be monotonic (w.r.t. the input function f); however, all points in π_1 and π_2 have function values within the range $[f(s_1), f(s_2)]$. The merging of π_1 and π_2 results in a new monotonic arc π_3 from s_1 and s_2, such that every point $p \in \text{im}\,\gamma$ is mapped to some $q \in \pi_3$ with $f(q) = f(p)$. See Fig. 3 (b) for an illustration.

Note that since a critical pair (m, s) (resp. an essential pair (s_1, s_2)) corresponds uniquely to a persistence pair $(f(m), f(s))$ in the ordinary persistence diagram (resp. $(f(s_1), f(s_2))$ in the extended persistence diagram), the above process also removes a point from the respective persistence diagram.

Let R and R' denote the Reeb graph before and after the simplification of a persistence pair $\tau = (b, d)$ by collapsing its corresponding branching or loop feature. Let π_1^τ and π_2^τ be as introduced above. Call $\gamma^\tau = \pi_1^\tau \cup \pi_2^\tau$ the *merging path w.r.t.* τ. Note that γ^τ is a closed curve corresponding to a thin cycle spanning (b, d) when it is an extended persistence pair, and a connected path with b and d being the respective minimum and maximum function values on it otherwise. In either case, the height of the merging path is at most $|d - b|$, the persistent of this pair (b, d). The merging path γ^τ will be collapsed into a single monotonic arc in order to eliminate the persistence pair τ. We can view the removal of τ in a more formal way as follows: We say that two points $x, y \in R$ are τ-equivalent, denoted by $x \sim_\tau y$, if $f(x) = f(y)$ and $x, y \in \gamma^\tau$. The simplified Reeb graph R' is the quotient space $R/\sim_\tau$; the corresponding quotient map $\mu_\tau : R \to R'$ satisfies $\mu_\tau(x) = \mu_\tau(y)$ if and only if $x \sim_\tau y$. The function $f : R \to \mathbb{R}$ induces a function $f' : R' \to \mathbb{R}$ such that for any $x' \in R'$, $f'(x') = f(x)$ for any $x \in \mu_\tau^{-1}(x')$.

Now given an input Reeb graph R, suppose we wish to eliminate a set of persistence pairs $\{\tau_1 = (b_1, d_1), \tau_2 = (b_2, d_2), \ldots, \tau_k = (b_k, d_k)\}$. Compute the merging path γ^{τ_i} for each persistence pair τ_i in R. We now define an equivalence relation $\sim$ as the transitive closure of all $\sim_{\tau_i}$s for $i \in [1, k]$. This is equivalent to collapsing γ^{τ_i}s for all $i \in [1, k]$ in an arbitrary order to kill the persistence pairs $\tau_1, \ldots, \tau_k$. The final simplified Reeb graph $\widetilde{R}$ is obtained as the quotient space $R/\sim$, with $\mu : R \to \widetilde{R}$ being the associated quotient map. We have a well-defined function $g : \widetilde{R} \to \mathbb{R}$ induced by the function $f : R \to \mathbb{R}$ such that $g(\mu(x)) = f(x)$ for any $x \in R$. Let δ denote the largest persistence of $\tau_1, \ldots, \tau_k$. We have the following properties of $\widetilde{R}$.

Observation 7.1. *(i) Given any two points $x, y \in R$, we have $d_g(\mu(x), \mu(y)) \leq d_f(x, y)$.*
(ii) Given a point $\tilde{x} \in \widetilde{R}$, for any two points $x_0, x_1 \in \mu^{-1}(\tilde{x})$ we have $d_f(x_0, x_1) \leq 2\delta$.

Proof. Claim (i) follows easily since the quotient map μ preserves function values. We now prove (ii). Since $\mu(x_0) = \mu(x_1) = \tilde{x}$, by the definition of μ there exists a set of equivalent relations $\sim_{\tau_{j_1}}, \ldots, \sim_{\tau_{j_a}}$ with the index set $\{j_1, \ldots, j_a\} \subseteq \{1, \ldots, k\}$ such that $y_0 := x_0 \sim_{\tau_{j_1}} y_1 \sim_{\tau_{j_2}} y_2 \cdots \sim_{\tau_{j_a}} y_a := x_1$. Set $\alpha = f(x_0) = f(x_1)$. All y_i have the same function value α. For each $i \in [1, a]$, we have that $y_{i-1} \sim_{\tau_{j_i}} y_i$, which is induced by the merging path $\gamma^{\tau_{j_i}}$ with $\text{height}(\gamma^{\tau_{j_i}}) \leq \delta$. In other words, there is a subpath π_i of $\gamma^{\tau_{j_i}}$ connecting y_{i-1} to y_i such that $\text{range}(\pi_i) \subseteq [\alpha - \delta, \alpha + \delta]$. The concatenation of these paths π_i gives rise to a path π connecting $y_0 = x_0$ and $y_a = x_1$, and $\text{range}(\pi) \subseteq [\alpha - \delta, \alpha + \delta]$. This proves claim (ii). $\qquad\square$

A similar argument of the above observation can in fact lead to the following more refined statements.

Lemma 7.2. *Let $y_a, y_b \in \widetilde{R}$ be two points in $\widetilde{R}$ such that there exists a monotonic path π^* between y_a and y_b with $d_g(y_a, y_b) = \text{height}(\pi^*) = g(y_b) - g(y_a)$, where $g(y_b) > g(y_a)$. Let x_a and x_b be arbitrary preimages for y_a and y_b, respectively. Then $d_f(x_a, x_b) \leq 2\delta + \text{height}(\tilde{\pi})$.*

In fact, there is a path π from x_a to x_b such that the highest point t in $\text{im}\,\pi$ satisfies $f(t) \leq f(x_b) + \delta$, and the lowest point w in $\text{im}\,\pi$ satisfies $f(w) \geq f(x_a) - \delta$.

7.2 Distance between R and $\widetilde{R}$

While the simplification scheme removes persistence pairs $\tau_1, \ldots, \tau_k$, it is not clear how other points in the persistence diagram of the original Reeb graph R are affected. In this section, we aim to bound the functional distortion distance $d_{FD}(R, \widetilde{R})$, which in turn will give an upper bound on the respective persistence diagrams. We do so through the functional Gromov-Hausdorff distance, $d_{fGH}(R, \widetilde{R})$, between R and $\widetilde{R}$. In particular, by using the quotient map $\mu : R \to \widetilde{R}$ which describes the simplification process implemented on R so that $\widetilde{R}$ is obtained, we will show that the functional Gromov-Hausdorff distance between R and $\widetilde{R}$ is bounded by δ.

First, we rewrite the definition of functional GH distance inEq. (7) by the following using the concept of correspondance: A correspondance $C \subset X \times Y$ between two topological spaces X and Y is a relation whose projection on X and on Y are both surjective. We can then rewrite Eq. (7) as follows:

$$D(C) = \frac{1}{2} \max_{(x_1, y_1), (x_2, y_2) \in C} |d_f(x_1, x_2) - d_g(y_1, y_2)|; \text{ and}$$

$$d_{fGH}(R, \widetilde{R}) = \inf_{C: R \times \widetilde{R}} \max\{D(C), \max_{(x,y) \in C} |f(x) - g(y)|\}, \tag{12}$$

where C ranges over all the correspondence between R and $\widetilde{R}$.

Set $\widehat{C} = \{(x, \mu(x)) | x \in R\}$. Note that this indeed is a correspondence since μ is a subjective map from R to $\widetilde{R}$. We will now bound $D(\widehat{C})$. Specifically, given any $\{(x_1, y_2), (x_2, y_2)\} \in \widehat{C}$ with $y_1 = \mu(x_1)$ and $y_2 = \mu(x_2)$, we aim to show that $|d_f(x_1, x_2) - d_g(y_1, y_2)| \leq 2\delta$; that is,

$$-2\delta \leq d_f(x_1, x_2) - d_g(y_1, y_2) \leq 2\delta \tag{13}$$

To see that the left inequality in Eq. (13) holds, note that by Observation 7.1, we have $d_g(y_1, y_2) - d_f(x_1, x_2) \leq 0$.
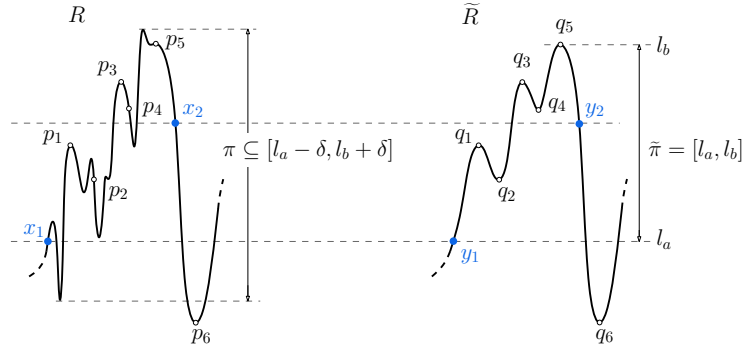

Figure 4: Right: An arc $(q_i, q_{i+1}) \in \widetilde{R}$ denotes a monotonic path. Each of them has a correspondent path $(p_i, p_{i+1}) \in R$, with $q_i = \phi(p_i)$. The path between y_1 and y_2 is the concatenation of a set of monotonic paths, i.e., $\tilde{\pi}(y_1, y_2) = \{(y_1, q_1,), \cdots, (q_5, y_2)\} \in \widetilde{R}$ with range$(\tilde{\pi}(y_1, y_2)) = [l_a, l_b]$. Left: There exists a path $\pi(x_1, x_2)$ in R, with x_1 and x_2 be the arbitrarily preimages of y_1 and y_2, respectively. The range of $\pi(x_1, x_2)$ can be bounded as $[l_a - \delta, l_b + \delta]$.

We now show the right part of Eq. (13). Assume w.l.o.g that the Reeb graph R and thus also $\widetilde{R}$ are connected. Let $\tilde{\pi}(y_1, y_2) \in \widetilde{R}$ denote the path with the minimum height connecting y_1 and y_2 (i.e, achieving $d_g(y_1, y_2)$) in $\widetilde{R}$. Suppose that $\tilde{\pi}(y_1, y_2) \in \widetilde{R}$ is the concatenation of a set of monotonic paths in $\widetilde{R}$; see Fig. 4:

$$\tilde{\pi}(y_1, y_2) = \{\tilde{\pi}(y_1 = q_0, q_1), \tilde{\pi}(q_1, q_2), \cdots, \tilde{\pi}(q_{s-1}, q_s = y_2)\} \in \widetilde{R}$$

20

By Lemma 7.2, each $\tilde{\pi}(q_i, q_{i+1})$ gives rise to a path $\pi(p_i, p_{i+1}) \in R$ such that $\mu(p_i) = q_i, \mu(p_{i+1}) = q_{i+1}$, and height($\pi^*(p_i, p_{i+1})) \leq 2\delta +$ height($\tilde{\pi}^*(q_i, q_{i+1})$). In fact, we can choose p_0 and p_s as x_1 and x_2 (which are preimages of y_1 and y_2), respectively. Concatenating all $\pi(p_i, p_{i+1})$, for $i = 0, \cdots, s$, we obtain a path $\pi(p_0 = x_1, p_s = x_2)$ with height($\pi(p_0, p_s)) \leq$ height($\tilde{\pi}(q_0, q_s)) + 2\delta$. Hence

$$d_f(x_1, x_2) \leq \text{height}(\pi(x_1 = p_0, x_2 = p_s)) \leq \text{height}(\tilde{\pi}(y_1 = q_0, y_2 = q_s)) + 2\delta = d_g(y_1, y_2) + 2\delta.$$

The right part of Eq. (13) thus holds. Hence $D(\widehat{C}) \leq \delta$.

Furthermore, since $\max_{(x,y) \in \widehat{C}} |f(x) - g(y)| = 0$ (as for any $y = \mu(x)$, $g \circ \mu(x) = f(x)$), we have that $d_{fGH}(R, \widetilde{R}) \leq \delta$. Therefore, by Theorem 5.1, we have

$$d_{FD}(R, \widetilde{R}) \leq 3d_{fGH}(R, \widetilde{R}) = 3\delta \tag{14}$$

Combining this with Theorems 4.2 and 4.3, we conclude with the following main result on the simplification of the Reeb graphs:

Theorem 7.3. *Suppose we simplify a Reeb graph R by removing features of persistence $\leq \delta$ using the strategy detailed in Section 7.1. The bottleneck distance between the (ordinary and extended) persistence diagrams for R and for its simplification $\widetilde{R}$ is at most 9δ.*

We remark that instead of invoking Theorem 5.1, one can use a direct argument similar to the proof of that theorem to improve the bound on $d_{FD}(R, \widetilde{R})$ to 2δ, which further improves the bound on bottleneck distance between persistence diagrams for R and $\widetilde{R}$ to 6δ.

8 Concluding Remarks

In this paper, we propose a distance for Reeb graphs, under which the Reeb graph is stable with respect to changes in the input function under the L_∞ norm. More importantly, we show that this distance is bounded from below by and thus more discriminative at differentiating scalar fields than the bottleneck distance between both 0th ordinary and 1st extended persistence diagrams. Similar to the Gromov-Hausdorff distance for metric spaces, the functional distortion distance provides a rigorous setting for describing and studying various properties of Reeb graphs. Indeed, by bounding the functional distortion distance between a Reeb graph and its simplification, we can prove that important (persistent) features are preserved under simplification, which addresses a key practical issue.

Our current bound in Theorem 4.3 has a constant factor of 3. It will be interesting to see whether this factor can be improved to 1 to match the bound in Theorem 4.2, either for the functional distortion distance or for some other distance.

A natural question is how to compute the functional distortion distance. We believe that there is an exponential time algorithm to approximate $d_{FD}(R_f, R_g)$, similar to what is known for the ε-interleaving distance for merge trees [28]. However, it remains an open problem to develop more efficient algorithms. We remark that comparing unlabeled trees is computationally hard in general: The commonly used tree edit distance and tree alignment distance are NP-hard to compute (and sometimes even to approximate) [8]. Similarly, it has been shown that computing the Gromov-Hausdorff distance is NP-hard even for two metric trees [2]. It will be interesting to see whether by leveraging the scalar field associated with merge trees and Reeb graphs, more efficient approximation algorithms for computing functional distortion distance can be developed.

Acknowledgements

References

[1] P. K. Agarwal, H. Edelsbrunner, J. Harer, and Y. Wang. Extreme elevation on a 2-Manifold. *Discrete Comput. Geom.*, 36(4):553–572, 2006.

[2] P. K. Agarwal, K. Fox, A. Nath, A. Sidiropoulos, and Y. Wang. Computing the Gromov-Hausdorff distance for metric trees. In *Proc. 26th Intl. Sympos. Algorithms and Computation (ISAAC)*, pages 529–540, 2015.

[3] U. Bauer and M. Lesnick. Induced matchings of barcodes and the algebraic stability of persistence. In *Proc. 30th Annu. ACM Sympos. Comput. Geom.*, 2014.

[4] U. Bauer, X. Ge, and Y. Wang. Measuring distance between Reeb graphs. In *Proceedings of the Thirtieth Annual Symposium on Computational Geometry - SoCG '14, Kyoto, Japan*, pages 464–473, 2014.

[5] U. Bauer, E. Munch, and Y. Wang. Strong equivalence of the interleaving and functional distortion metrics for Reeb graphs. In *Sympos. Comput. Geom. (SoCG)*, pages 461–475, 2015.

[6] K. Beketayev, D. Yeliussizov, D. Morozov, G. H. Weber, and B. Hamann. Measuring the distance between merge trees. In *TopoInVis'13*, 2013.

[7] S. Biasotti, D. Giorgi, M. Spagnuolo, and B. Falcidieno. Reeb graphs for shape analysis and applications. *Theor. Comput. Sci.*, 392(1-3):5–22, 2008.

[8] P. Bille. A survey on tree edit distance and related problems. *Theor. Comput. Sci.*, 337(1-3):217–239, 2005.

[9] G. Carlsson and V. de Silva. Zigzag persistence. *Foundations of Computational Mathematics*, 10(4): 367–405, 2010.

[10] F. Chazal and J. Sun. Gromov-Hausdorff approximation of filament structure using Reeb-type graph. In *Proc. 30th Annu. ACM Sympos. Compu. Geom., To appear*, 2014.

[11] F. Chazal, D. Cohen-Steiner, M. Glisse, L. J. Guibas, and S. Oudot. Proximity of persistence modules and their diagrams. In *Proc. 25th ACM Sympos. on Comput. Geom.*, pages 237–246, 2009.

[12] F. Chazal, D. C. Steiner, L. J. Guibas, F. Mémoli, and S. Y. Oudot. Gromov-Hausdorff stable signatures for shapes using persistence. In *Proceedings of the Symposium on Geometry Processing*, SGP '09, pages 1393–1403. Eurographics Association, 2009.

[13] F. Chazal, V. de Silva, M. Glisse, and S. Oudot. The structure and stability of persistence modules. Preprint, 2012. `arXiv:1207.3674`.

[14] D. Cohen-Steiner, H. Edelsbrunner, and J. Harer. Stability of persistence diagrams. *Discrete Comput. Geom.*, 37(1):103–120, 2007.

[15] D. Cohen-Steiner, H. Edelsbrunner, and J. Harer. Extending persistence using Poincaré and Lefschetz duality. *Foundations of Computational Mathematics*, 9(1):79–103, 2008.

[16] V. de Silva, E. Munch, and A. Patel. Categorification of reeb graphs. Preprint, 2014.

[17] T. Dey and Y. Wang. Reeb graphs: Approximation and persistence. *Discrete Comput. Geom.*, 49(1): 46–73, 2013.

[18] B. Di Fabio and C. Landi. Stability of Reeb graphs of closed curves. *Electronic Notes in Theoretical Computer Science*, 283:71–76, 2012.

[19] H. Doraiswamy and V. Natarajan. Output-sensitive construction of Reeb graphs. *IEEE Trans. Vis. Comput. Graph.*, 18(1):146–159, 2012.

[20] H. Edelsbrunner and J. Harer. *Computational Topology: An Introduction*. Amer. Math. Soc., Providence, Rhode Island, 2009.

[21] H. Edelsbrunner, D. Letscher, and A. Zomorodian. Topological persistence and simplification. *Discrete Comput. Geom.*, 28(4):511–533, 2002.

[22] X. Ge, I. Safa, M. Belkin, and Y. Wang. Data skeletonization via Reeb graphs. In *Proc. 25th Annu. Conf. Neural Infor. Process. Sys. (NIPS)*, pages 837–845, 2011.

[23] W. Harvey, R. Wenger, and Y. Wang. A randomized $O(m \log m)$ time algorithm for computing Reeb graph of arbitrary simplicial complexes. In *Proc. 25th Annu. ACM Sympos. Compu. Geom.*, pages 267–276, 2010.

[24] A. Hatcher. *Algebraic Topology*. Cambridge University Press, 2002.

[25] F. Hétroy and D. Attali. Topological quadrangulations of closed triangulated surfaces using the Reeb graph. *Graph. Models*, 65(1-3):131–148, 2003.

[26] M. Hilaga, Y. Shinagawa, T. Kohmura, and T. L. Kunii. Topology matching for fully automatic similarity estimation of 3D shapes. In *Proc. SIGGRAPH '01*, pages 203–212, 2001.

[27] N. J. Kalton and M. I. Ostrovskii. Distances between Banach spaces. *Forum Mathematicum*, 11(1), 2008.

[28] D. Morozov, K. Beketayev, and G. Weber. Interleaving distance between merge trees, 2013. Manuscript.

[29] M. Natali, S. Biasotti, G. Patanè, and B. Falcidieno. Graph-based representations of point clouds. *Graphical Models*, 73(5):151 – 164, 2011.

[30] S. Parsa. A deterministic $O(m \log m)$ time algorithm for the Reeb graph. In *Discrete Comput. Geom.*, volume 49, pages 864–878. Springer-Verlag, 2013.

[31] V. Pascucci, G. Scorzelli, P.-T. Bremer, and A. Mascarenhas. Robust on-line computation of Reeb graphs: simplicity and speed. *ACM Trans. Graph. (SIGGRAPH 2007)*, 26(3), 2007.

[32] G. Reeb. Sur les points singuliers d'une forme de Pfaff complètement intégrable ou d'une fonction numérique. *Comptes Rendus Hebdomadaires des Séances de l'Académie des Sciences*, 222:847–849, 1946.

[33] Y. Shinagawa, T. Kunii, and Y. L. Kergosien. Surface coding based on Morse theory. *IEEE Comput. Graph. Appl.*, 11(5):66–78, 1991.

[34] G. Singh, F. Mémoli, and G. Carlsson. Topological methods for the analysis of high dimensional data sets and 3D object recognition. In *Eurograph. Sympos. Point-Based Graphics*, pages 91–100, 2007.

[35] J. Tierny. *Reeb graph based 3D shape modeling and applications*. PhD thesis, Université des Sciences et Technologies de Lille, 2008.

[36] J. H. van Lint and R. M. Wilson. *A course in Combinatorics*. Cambridge Univerisity Press, 1992.

[37] Z. Wood, H. Hoppe, M. Desbrun, and P. Schröder. Removing excess topology from isosurfaces. *ACM Trans. Graph.*, 23(2):190–208, 2004.

[38] A. Zomorodian and G. Carlsson. Computing persistent homology. *Discrete Comput. Geom.*, 33(2): 249–274, 2005.